Eur. J. Mineral., 38, 75–101, 2026
https://doi.org/10.5194/ejm-38-75-2026

European Journal of Mineralogy
Open Access

Crystal structure, chemical composition, and twinning of götzenite and wöhlerite from the Fohberg phonolite, Kaiserstuhl

Reinhard X. Fischer[1], Johannes Birkenstock[1], Georg Biskup[2], Lennart A. Fischer[3], Andreas Klügel[1], Shaghayegh Nezamabadi[1], and Simon Spürgin[4]

[1]Fachbereich Geowissenschaften, Universität Bremen, 28359 Bremen, Germany
[2]independent researcher: Pforzheim, Germany
[3]Institut für Geo- und Umweltwissenschaften, Geochemie, Albert-Ludwigs-Universität, Freiburg, Germany
[4]Hans G. Hauri KG, Bötzingen, Germany

Correspondence: Reinhard X. Fischer (rfischer@uni-bremen.de)

Received: 5 August 2025 – Revised: 26 December 2025 – Accepted: 14 January 2026 – Published: 24 February 2026

Abstract. Götzenite and wöhlerite were found as part of a fissure assemblage in the Fohberg phonolite (Kaiserstuhl, SW Germany), in close association with natrolite and clinopyroxene (aegirine–augite). Crystal grains were separated and investigated by single-crystal X-ray diffraction (SXRD), electron probe microanalysis (EPMA), and laser ablation inductively coupled plasma mass spectrometry (LA-ICP-MS), showing the presence of two intimately intergrown phases, götzenite and wöhlerite. SXRD analyses showed that both minerals are twinned. Götzenite ($Na_{1.50}Ca_{5.18}Sr_{0.13}Fe^{2+}_{0.03}Mn_{0.01}Zr_{0.06}La_{0.08}Ce_{0.11}Nd_{0.02}Ti_{0.81}Nb_{0.19}(Si_2O_7)_2O_{1.2}F_{2.8}$) shows rotation twinning on [001] according to $-\boldsymbol{a} - 1/2\boldsymbol{c}$, $-\boldsymbol{b}$, $\boldsymbol{c}$, with contributions of 40 % and 60 % from the two twin domains, respectively. Applying the twin law to the diffraction analysis, the crystal structure was refined to $R1\ (Fo > 4\sigma\ (Fo)) = 3.0\,\%$, with $a = 9.6191(3)$ Å, $b = 5.7342(2)$ Å, $c = 7.3386(2)$ Å, $\alpha = 89.986(1)°$, $\beta = 101.040(1)°$, $\gamma = 100.485(1)°$, and $V = 390.40(3)$ Å^3 in space group $P\,\overline{1}$. Wöhlerite ($Na_{1.63}Ca_{4.37}Sr_{0.04}Zr_{0.63}Fe^{2+}_{0.23}Mn_{0.09}Ce_{0.01}Ta_{0.01}Nb_{0.79}Ti_{0.20}(Si_2O_7)_2O_{2.6}F_{1.4}$) shows reflection twinning on (100) according to $-\boldsymbol{a} - \boldsymbol{c}$, $\boldsymbol{b}$, $\boldsymbol{c}$, with contributions of 31 % and 69% from the two twin domains, respectively, and with lattice parameters of $a = 10.842(1)$ Å, $b = 10.249(1)$ Å, $c = 7.2673(8)$ Å, $\beta = 109.343(4)°$, and $V = 761.9(2)$ Å^3 in the monoclinic space group $P2_1$, refined to $R1 = 1.3\,\%$. Refractive indices of götzenite were measured using the immersion method yielding $n_x = 1.662(2)$, $n_y = 1.663(2)$, $n_z = 1.670(2)$, and $2V = 61(2)°$. Optical measurements on the twinned crystal were possible because of the coincidence of the two indicatrices related to each other by rotation about n_x being parallel to [001], simulating a unique extinction behavior. Wöhlerite could not be optically examined because of the polysynthetic twinning not showing this effect.

1 Introduction

1.1 Occurrence

Götzenite and wöhlerite were found in a phonolite sample from the Kaiserstuhl Volcanic Complex (SW Germany). The sample was collected in 2019 in the quarry operated by Hans G. Hauri KG Mineralstoffwerke in Bötzingen, Germany, which exposes the Miocene, subvolcanic, intrusive Fohberg phonolite. Both minerals were found as part of a fissure assemblage, having a similar appearance with yellowish brown, prismatic, or lath-like crystals, as shown in Fig. 1.

Götzenite and wöhlerite occur as intergrown crystals in the same aggregates and are visually indistinguishable. Associated minerals in the fissure are natrolite and clinopyroxene (aegirine–augite). Götzenite was first recognized in the Fohberg phonolite as part of the rock matrix by Czygan (1973) and is known to have formed during the magmatic crystallization stage (Weisenberger et al., 2014). Spürgin et al. (2024) investigated the chemical composition of götzen-

Figure 1. Yellowish-brown crystals of götzenite and wöhlerite in association with natrolite (white) and clinopyroxene (black). The widths of the figures are 11 cm (top) and 5.7 mm (bottom), respectively.

ite from the rock matrix and found a strong enrichment in rare earth elements (REEs), Na, Zr, and especially Nb in later crystallized grains, whereas early-formed crystals show compositions close to the ideal mineral formula. However, non-matrix crystals of götzenite in large (centimeter-sized) aggregates from fissure assemblages were not known at this point from the Fohberg phonolite. Furthermore, wöhlerite has not been reported from this locality before. Mineralogical and petrological descriptions of the Fohberg phonolite are given by Weisenberger et al. (2014) and Spürgin et al. (2019).

1.2 Systematics

1.2.1 Götzenite

Götzenite, ideally $NaCa_6Ti(Si_2O_7)_2OF_3$ (Sokolova and Cámara, 2013), belongs to the rinkite group of minerals (Christiansen et al. (2003a) have named this group the rosenbuschite group; in Sokolova (2006) and Sokolova and Cámara (2013), it is Group I) in the seidozerite supergroup of TS-block (TS denotes titanium silicate) minerals (Sokolova and Cámara, 2017). The TS block consists of a central octahedral sheet O and two adjacent heteropolyhedral sheets H. These HOH layers are characteristic sheets of minerals in the polysomatic series of heterophyllosilicates, as described by Ferraris (2008). Here, we follow

the classification based on the crystallographic description of the titanosilicates with TS blocks, as described by Sokolova (2006). The general formula of the TS block is $A^P_2B^P_2M^H_2M^O_4(Si_2O_7)_2X_{4+n}$, with the cations M^H_2 of the H sheet; the cations M^O_4 of the O sheet; A^P and B^P cations at peripheral (P) sites; and $X_{4+n} = 4X^O + nX^P$, with the apical anions $X^P = X^P_M + X^P_A$ at the periphery of the TS block (see Eq. 10 in Sokolova, 2006, and Sokolova and Cámara, 2013, 2017). Thus, the ideal structural formula of götzenite can be described as $A^P_2 = Ca_2$; $M^H_2 = Ca_2$; $M^O_4 = NaCa_2Ti$; $(Si_2O_7)_2$; and $X^O = X^O_M + X^O_A$, with $(X^O_M)_2 = (OF)$ and $(X^O_A)_2 = F_2$. Rinkite-group minerals including götzenite are characterized as having a fixed content of 1 apfu in the Ti-bearing site (Ti + Nb in götzenite) normalized to one unit of $(Si_2O_7)_2$ (Sokolova and Cámara, 2013, 2017; Day et al., 2022). Götzenite was first described by Sahama and Hytönen (1957) from a nephelinite of the extinct Mt. Shaheru volcano (Democratic Republic of Congo). It was observed that almost every crystal showed lamellar twinning with the twin axis ***b***, which in the unit cell setting used here, corresponds to axis ***c***. Fleischer (1958a, b) pointed out in his discussion that the minerals götzenite and Ca rinkite appear to be identical, and Sahama (1960) has proven that the calcium rinkite described by Slepnev (1957) is identical to götzenite and "may be termed a rare earth- and niobium-bearing strontian götzenite". The structural relationship between götzenite and rinkite is discussed by Christiansen and Rønsbo (2000). Consequently, the name Ca rinkite was discredited by the Commission on New Minerals and Mineral Names of the International Mineralogical Association (Min. Mag. 33, 1962, 260–263). Under this aspect, the occurrence of götzenite termed Ca rinkite was mentioned by Chirvinskiy (1935) and Starynkevich-Borneman (1935), quoted after Val'ter et al. (1963). Neumann (1962) and Sahama et al. (1966) discussed the close relationship between rosenbuschite and götzenite by comparing the X-ray powder diffraction data and chemical compositions. The crystal structure of götzenite was solved by Cannillo et al. (1972) on a twinned crystal from Mt. Shaheru (Democratic Republic of Congo). It is closely related to the other rinkite-group minerals rinkite–Ce) $Na_2Ca_4(REE)Ti(Si_2O_7)_2OF_3$ (Cámara et al., 2011; Sokolova and Cámara, 2017), rinkite-(Y) $Na_2Ca_4YTi(Si_2O_7)_2OF_3$ (Pautov et al., 2019), nacareniobsite-(Ce) $Na_3Ca_3(REE)Nb(Si_2O_7)_2OF_3$ (Sokolova and Hawthorne, 2008), mosandrite-(Ce) $(Ca_3REE)[(H_2O)_2Ca_{0.5}\square_{0.5}]Ti(Si_2O_7)_2(OH)_2(H_2O)_2$ (Sokolova and Hawthorne, 2013; Sokolova and Cámara, 2017), seidozerite $Na_4MnZr_2Ti(Si_2O_7)_2O_2F_2$ (Christiansen et al., 2003a), grenmarite $Na_4MnZr_3(Si_2O_7)_2O_2F_2$ (Bellezza et al., 2004a; Sokolova and Cámara, 2017), hainite-(Y) $Na_2Ca_4YTi(Si_2O_7)_2OF_3$ (Lyalina et al., 2015; Sokolova and Cámara, 2017), fogoite-(Y) $Na_3Ca_2Y_2Ti(Si_2O_7)_2OF_3$ (Cámara et al., 2017), batievaite-(Y) $Ca_2Y_2Ti(Si_2O_7)_2(OH)_2(H_2O)_4$ (Lyalina et al., 2016), kochite $Na_3Ca_2MnZrTi(Si_2O_7)_2OF_3$ (Christiansen et al., 2003b; Sokolova and Cámara, 2017), rosenbuschite $Na_6Ca_6Zr_3Ti(Si_2O_7)_4O_2F_6$ (Christiansen et al., 2003a; Sokolova and Cámara, 2017), and bortolanite $Na_2Ca_{4.5}Zr_{0.5}Ti(Si_2O_7)_2OF_3$ (Day et al., 2022). In particular, the members fogoite-(Y), batievaite-(Y), hainite-(Y), and bortolanite are closely related to götzenite, all being triclinic in space group $P\bar{1}$ with similar lattice parameters. The following criteria are used to distinguish between götzenite and the related minerals. In fogoite-(Y), Ca is replaced by Y in the H sheet of götzenite and by Na in the O sheet. In batievaite-(Y), Ca is replaced by Y in the H sheet of götzenite, and the Na site in the O sheet is essentially vacant. Hainite-(Y) differs from götzenite by containing more Na and Y, which occupy separate sites in the crystal structure (Lyalina et al., 2015). In bortolanite, 0.5 Ca in the H sheet of götzenite is replaced by Zr, and Ca in the O sheet is replaced by Na (Day et al., 2022).

1.2.2 Wöhlerite

Wöhlerite, ideally $Na_2Ca_4ZrNb(Si_2O_7)_2O_3F$ (Dal Bo et al., 2022), was first described by Scheerer (1843). The mineral was found on Løvøya Island close to the city of Brevig in Norway. Chemical analysis revealed a silicate containing mainly Na, Ca, Zr, and Nb, with minor amounts of Mg, Mn, and Fe, where Nb was erroneously given as Ta, as discussed by Dal Bo et al. (2022). Following Biagioni et al. (2012) and Dal Bo et al. (2022), wöhlerite belongs to a group of minerals usually named the wöhlerite group but sometimes also designated as the cuspidine group (Merlino and Perchiazzi, 1988; see Dal Bo et al., 2022, for details), with the general composition $X_8(Si_2O_7)_2W_4$. Other members (for references, see Dal Bo et al., 2022) besides wöhlerite are cuspidine $Ca_8(Si_2O_7)_2F_4$, låvenite $Na_2Ca_2Mn_2Zr_2(Si_2O_7)_2O_2F_2$, normandite $Na_2Ca_2Mn_2Ti_2(Si_2O_7)_2O_2F_2$, niocalite $Ca_7Nb(Si_2O_7)_2O_3F$, janhaugite $Na_3Mn_3Ti_2(Si_2O_7)_2(OH)_2OF$, burpalite $Na_4Ca_2Zr_2(Si_2O_7)_2F_4$, baghdadite $Ca_6Zr_2(Si_2O_7)_2O_4$, hiortdahlite $Na_2Ca_4(Ca_{0.5}Zr_{0.5})Zr(Si_2O_7)_2OF_3$, moxuanxueite $NaCa_6Zr(Si_2O_7)_2OF_3$, madeiraite $Na_2Ca_2Fe_2Zr_2(Si_2O_7)_2O_2F_2$ (Mills et al., 2021), and pilanesbergite $Na_2Ca_2Fe_2Ti_2(Si_2O_7)_2O_2F_2$ (Dal Bo et al., 2024). Goßner and Kraus (1933) determined the lattice parameters and assigned space group $P2_1$ or $P2_1/m$ to wöhlerite, with a preference for the latter. Shibaeva and Belov (1962) solved the crystal structure representing a sorosilicate with cation polyhedra linked by Si_2O_7 groups. A detailed refinement of the crystal structure was done by Mellini and Merlino (1979). The mineral marianoite (Chakhmouradian et al., 2008) was discredited because it was found to be equivalent to wöhlerite (Miyawaki et al., 2020; Dal Bo et al., 2022; see also the discussion by Merlino and Mellini, 2009, and Chakhmouradian and Mitchell, 2009). Wöhlerite was also identified in a multi-phase mineral species named "guarinite", consisting of three

distinct domains with hiortdahlite II in domain I, wöhlerite in domain II, and hiortdahlite I in domain IV (Bellezza et al., 2012).

2 Experimental methods

2.1 Chemical analyses

2.1.1 Tasks

In order to support the identification of the mineral species investigated by X-ray diffraction methods and to provide possible models for the cation distribution in the crystal structure, chemical analyses were done by electron probe microanalyses (EPMA) using two different instruments at the University of Freiburg (UF) and the University of Bremen (UB). The first analysis at UF yielded a chemical composition close to that of wöhlerite which did not match the identification of the mineral by X-ray diffraction (XRD), indicating a götzenite-like species. This prompted us to search for another crystal with a similar appearance. Finally, several crystals could be separated among which both götzenite and wöhlerite could be identified. Both phases were analyzed by EPMA at UB. Since the sum of the weight fractions was significantly lower than 100 %, additional analyses were done using laser ablation inductively coupled plasma mass spectrometry (ICP-MS) to determine the contents of elements not routinely analyzed by EPMA.

2.1.2 Electron probe microanalysis (EPMA)

Götzenite and wöhlerite crystals were analyzed at the Institut für Geo- und Umweltwissenschaften (University of Freiburg, UF) and the Faculty of Geosciences (University of Bremen, UB), each with a Cameca SX 100 equipped with five wavelength dispersive spectrometers (WDSs). Analytical conditions included 15 kV acceleration voltage, 15 nA beam current, and a focused beam (1 µm) at Freiburg and a 15 kV/20 nA/5 µm at Bremen, respectively. Raw data were corrected with the software PeakSight™ using the built-in PAP matrix correction (Pouchou and Pichoir, 1991). Spectrometer crystals and calibration standards are listed in Table 1. Figure 2 shows the back-scattered electron (BSE) image of a sample region where wöhlerite and götzenite are in direct contact with each other.

2.1.3 Laser ablation inductively coupled plasma mass spectrometry (LA-ICP-MS)

Laser ablation (LA) ICP-MS analyses of Rb, Y, Ba, rare earth elements (REE), Hf, Ta, Pb, Th, and U were carried out on a polished slice using a NewWave UP193ss laser coupled to a Thermo Element 2 at the Faculty of Geosciences, University of Bremen. Ablation was done with a laser pulse rate of 5 Hz, an irradiance of $\sim 1\,\mathrm{GW\,cm^{-2}}$, and circular spots of 35 or 50 µm diameter for samples and 75 µm for standards. Helium ($\sim 0.8\,\mathrm{L\,min^{-1}}$) was used as the carrier gas, and argon ($\sim 0.8\,\mathrm{L\,min^{-1}}$) was added as the make-up gas; the plasma power was 1200 W. All isotopes were analyzed at low resolution with five samples in a 20 % mass window and with a total dwell time of 25 ms per isotope. Oxide formation was low ($\mathrm{ThO/Th} \leq 0.1$ %) so that no mass interference corrections were applied. The analyses were quantified using the Cetac GeoProTM software with NIST610 glass standard reference material (SRM) for external calibration and with Ca as the internal standard element. The Ca concentrations of the samples were derived from the previous EPMA analyses. Accuracy was monitored by analyses of the USGS basalt glasses BHVO-2G and BCR-2G (Jochum et al., 2005), along with the samples.

2.1.4 Chemical composition

The results of the electron probe microanalysis (EPMA, wt %) and the laser ablation spectrometry analyses (LA-ICP-MSs, $\mu g\,g^{-1}$) are listed in Table 2. The major element concentrations are principally in accordance with the ideal end-member compositions if some allowance is made for cation exchanges such as Ti–Zr, Ti–Nb, or Ca–Sr. The low totals of the EPMA analyses are largely explained by the high concentrations of trace elements not analyzed, such as the rare earth elements ($\sum$REE = 2.58 wt %–4.18 wt % in götzenite and 0.23 wt %–0.44 wt % in wöhlerite); Ta, Th, and U in götzenite; and Hf, Ta, and U in wöhlerite. The high REE and Sr contents of götzenite suggest substantial replacement of Ca^{2+} by Sr^{2+} and REE^{3+}, with the latter possibly being a coupled substitution of $2\,Ca^{2+} <=> REE^{3+} + Na^{+}$, which might explain the relatively low Ca and high Na contents of götzenite when compared to the ideal composition and to the composition of wöhlerite (see Table 2). The chondrite-normalized REE spectra of götzenite show a weak s shape with systematic enrichment of the lighter REE relative to the heavier REE. Those of wöhlerite show a pronounced s shape with a maximum at La and Ce, a minimum at Ho, and a gradual increase from Er to Lu (Fig. 3). The weight fractions of the main elements and trace elements obtained from EPMA and LA-ICP-MS, respectively, are listed in Table S1 in the Supplement. The formula units calculated from the weight fractions listed in Tables 2 and S1 are presented in Table 3, scaled to four Si atoms (two Si_2O_7 groups) per unit cell.

2.2 Single-crystal X-ray diffraction

2.2.1 Instrumental settings and crystal data

Single-crystal X-ray diffraction (SXRD) measurements of götzenite and wöhlerite crystals were carried out on a Bruker D8 Venture diffractometer using MoKα radiation ($\lambda = 0.71076$ Å) at the University of Bremen, Fachbereich Geowissenschaften. The instrument is equipped with a curved TRIUMPH monochromator, a 0.3 mm collimator, a

Table 1. Spectrometer crystals and calibration standards.

Element	F	Na	Si	Ca	Ti
Bremen	PC1, fluorite	TAP, anorthoclase	TAP, diopside	PET, diopside	PET, ilmenite
Freiburg	PC1, fluorite	TAP, albite	TAP, wollastonite	PET, wollastonite	PET, rutile
Element	Mn	Fe	Sr	Zr	Nb
Bremen	LLIF, ilmenite	LLIF, hypersthene	TAP, strontianite	TAP, zircon	LPET, ilmenite
Freiburg	LIF, spessartine	LIF, hematite	TAP, Sr–Nb–phosphate	TAP, zircon	PET, Sr–Nb–phosphate

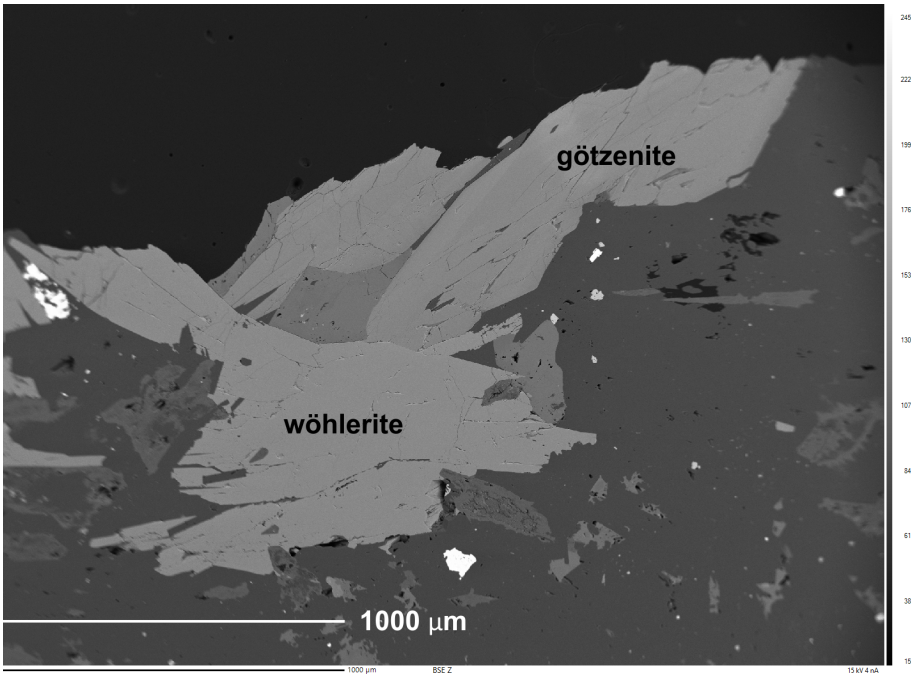

Figure 2. BSE image of götzenite and wöhlerite.

four-circle goniometer in κ geometry, and a Photon 100 (götzenite data) or a Photon III (wöhlerite data) CMOS area detector. Data collection parameters and single-crystal data are listed in Table 4.

Structure refinements were done with the program SHELX-97 (Sheldrick, 1997, 2008) as part of the WINGX suite (Farrugia, 1999) using scattering factors of the neutral elements. If possible, the occupancies of atoms were refined or they were fixed to the values determined from the chemical analyses if more than two elements with minor amounts were sharing one site. Crystal structure projections were drawn with the program STRUPLO (Fischer and Messner, 2025). Some entries with atom parameters were taken from the Inorganic Crystal Structure Database (ICSD; Belsky et al., 2002) when the atom parameters were not available in the original publications.

Bond valences (bond strengths) s_{ij} for pairs of cations i and anions j are calculated with the program VaList (Wills, 2018) according to the relation

$$s_{ij} = e^{\frac{R_0 - R_{ij}}{B}}, \quad (1)$$

with the bond length R_{ij} and the empirical parameters R_o and B listed in Table 5, as used for the calculations in Sect. 4. It should be noted that bond valence values might be erroneous if they are calculated for mixed occupancies at cation and/or anion sites, as discussed by Bosi (2014). Systematic errors might be introduced by using the mean distances R_{ij} in Eq. (1) resulting from the simultaneous refinement of the positional parameters of different atoms on the same site which are, in fact, displaced from the mean position with different bond lengths to the next neighbors in the local environment. However, the averaged bond valence values listed in Sect. 4.1 for götzenite and in Sect. 4.2 for wöhlerite can still be used as a rough guide to assess the choice of cations and anions at a certain site.

Table 2. EPMA (wt %) and LA-ICP-MS (µg g^{-1}) results obtained at the University of Bremen (UB) and the University of Freiburg (UF).

	EPMA				LA-ICP-MS					
	Götzenite	Wöhlerite			Götzenite	Wöhlerite		Götzenite	Wöhlerite	
	UB	UF	UB		UB	UB		UB	UB	
No. of spots	41	16	32		5	5		5	5	
Na_2O	5.79(22)	6.28(24)	6.24(19)	Rb	0.33(20)	0.9(8)	Dy	28(17)	17(4)	
MnO	0.13(4)	0.77(6)	0.80(5)	Y	188(75)	180(34)	Ho	4(3)	3.5(7)	
FeO	0.23(10)	2.08(14)	2.06(17)	Ba	127(10)	12(5)	Er	12(7)	13(2)	
SiO_2	29.93(48)	30.08(32)	29.50(25)	La	13197(2210)	701(209)	Tm	1.6(8)	2.3(4)	
ZrO_2	0.87(35)	9.57(58)	9.74(36)	Ce	19702(4005)	1707(519)	Yb	11(5)	22(3)	
SrO	1.71(39)	0.48(8)	0.45(9)	Pr	1402(260)	162(49)	Lu	1.5(5)	4.0(6)	
CaO	36.18(109)	30.84(53)	29.95(58)	Nd	2937(303)	461(141)	Hf	29(6)	484(4)	
TiO_2	7.98(76)	2.03(37)	1.92(37)	Sm	168(27)	42(13)	Ta	437(159)	2469(235)	
Nb_2O_5	2.90(99)	12.67(36)	13.35(60)	Eu	31(9)	9(3)	Pb	7.0(7)	3.9(4)	
F	8.38(30)	2.80(15)	3.61(24)	Gd	62(26)	23(6)	Th	1945(640)	170(49)	
total	94.10	97.53	97.63	Tb	6(3)	2.9(7)	U	712(53)	438(25)	

Table 3. Formula units corresponding to atoms per unit cell. UF denotes University of Freiburg, and UB denotes University of Bremen.

	Götzenite	Wöhlerite			Götzenite	Wöhlerite		Götzenite	Wöhlerite
	UB	UF	UB		UB	UB		UB	UB
Ca	5.18(11)	4.39(19)	4.35(7)	Rb	0.000003(2)	0.000008(8)	Dy	0.00014(9)	0.00009(2)
Na	1.50(7)	1.62(9)	1.64(5)	Y	0.002(1)	0.0016(3)	Ho	0.00002(1)	0.000017(3)
Mn	0.014(4)	0.087(8)	0.09(1)	Ba	0.0008(1)	0.00007(3)	Er	0.00006(3)	0.00006(1)
Fe	0.03(1)	0.23(2)	0.23(2)	La	0.08(1)	0.004(1)	Tm	0.000008(4)	0.000011(2)
Si	4	4	4	Ce	0.11(2)	0.010(3)	Yb	0.00005(2)	0.00010(2)
Zr	0.06(2)	0.62(5)	0.64(2)	Pr	0.008(2)	0.0009(3)	Lu	0.000007(3)	0.000018(3)
Sr	0.13(3)	0.037(6)	0.04(1)	Nd	0.017(2)	0.0026(8)	Hf	0.00013(3)	0.00218(2)
Ti	0.80(7)	0.20(4)	0.20(4)	Sm	0.0008(1)	0.00022(7)	Ta	0.0020(7)	0.012(1)
Nb	0.18(6)	0.76(4)	0.82(4)	Eu	0.00015(4)	0.00005(1)	Pb	0.000027(3)	0.000015(2)
O	14.48(12)	16.50(1)	16.48(12)	Gd	0.0003(1)	0.00012(3)	Th	0.007(2)	0.0006(2)
F	3.54(18)	1.18(8)	1.55(10)	Tb	0.00003(2)	0.000014(3)	U	0.0024(2)	0.0015(1)

2.2.2 Crystal structure determination

Götzenite

Crystals were prepared from the yellowish-brown part of the rock shown in Fig. 1. Only fragments could be separated with an anhedral shape not allowing routine identification. A fragment showing uniform extinctions under the polarizing microscope was selected and mounted on a goniometer head for single-crystal X-ray diffraction. Inspection of sections in reciprocal space (calculated with Bruker APEX2 instrument control software) yielded a preliminary C-centered monoclinic unit cell with space group $C2/m$ and lattice parameters $a = 37.346(2)$ Å, $b = 7.3299(3)$ Å, $c = 5.7259(2)$ Å, and $\beta = 96.866°$. Attempts to solve the crystal structure yielded rosenbuschite-like fragments with Si_2O_7 groups linked by MO_6 octahedra in a disordered arrangement where two components seemed to overlap. The $R1$ residual could not be refined below about 18 %. A possible explanation was the presence of twinning. Based on this hypothesis, a smaller unit cell with triclinic symmetry was found, which could be derived from the monoclinic unit cell according to the transformation $1/4\ (\boldsymbol{a}+\boldsymbol{b})$, $\boldsymbol{c}$, $-\boldsymbol{b}$. Refinement of lattice parameters after data collection in the triclinic setting yielded $a = 9.6191(3)$ Å, $b = 5.7342(2)$ Å, $c = 7.3386(2)$ Å, $\alpha = 89.986(1)°$, $\beta = 101.040(1)°$, and $\gamma = 100.485(1)°$ in space group $P\bar{1}$ with rotation twinning on [001] according to (−0.99997, 0.00023, −0.50199; −0.00008, −1.00002, 0.00034; −0.00001, −0.00002, 1.00000), which is close to the vector representation $-\boldsymbol{a} - 1/2\boldsymbol{c}$, $-\boldsymbol{b}$, $\boldsymbol{c}$, with contributions of 40 % and 60 % from the two twin domains, respectively. Based on these lattice parameters and on the structural fragments found in the structure determination, the mineral could be identified as götzenite, though it was closely related to other species in the rinkite group of minerals as well (see the discussion in Sect. 4.1). We cross-checked the derived twinning law for rotation twinning on [001] with the soft-

Table 4. Data collection parameters, refinement details, and crystal data.

Crystal data	Götzenite	Wöhlerite
Chemical composition from EPMA	$Na_{1.50}Ca_{5.18}Sr_{0.13}Fe_{0.03}Mn_{0.01}Zr_{0.06}La_{0.08}Ce_{0.11}Nd_{0.02}Ti_{0.80}Nb_{0.18}(Si_2O_7)_2O_{0.9}F_{3.5}$	$Na_{1.63}Ca_{4.37}Sr_{0.04}Zr_{0.63}Fe_{0.23}Mn_{0.09}Ce_{0.01}Ta_{0.01}Nb_{0.79}Ti_{0.20}(Si_2O_7)_2O_{2.54}F_{1.37}$
Chemical composition from SXRD[a]	$Na_{1.42}Ca_{5.15}Sr_{0.13}Fe_{0.03}Mn_{0.01}Zr_{0.06}La_{0.07}Ce_{0.11}Nd_{0.02}Ti_{0.94}Nb_{0.06}(Si_2O_7)_2O_{0.90}F_{3.10}$	$Na_{1.72}Ca_{4.28}Zr_{0.59}Fe_{0.32}Mn_{0.09}Nb_{0.78}Ti_{0.22}(Si_2O_7)_2O_{2.77}F_{1.23}$
Chemical composition used[a]	$Na_{1.50}Ca_{5.18}Sr_{0.13}Fe_{0.03}Mn_{0.01}Zr_{0.06}La_{0.08}Ce_{0.11}Nd_{0.02}Ti_{0.81}Nb_{0.19}(Si_2O_7)_2O_{1.2}F_{2.8}$	$Na_{1.63}Ca_{4.37}Sr_{0.04}Zr_{0.63}Fe^{2+}_{0.23}Mn_{0.09}Ce_{0.01}Ta_{0.01}Nb_{0.79}Ti_{0.20}(Si_2O_7)_2O_{2.6}F_{1.4}$
Space group	$P\,\bar{1}$	$P\,2_1$
Z	1	2
a (Å)	9.6191(3)	10.842(1)
b (Å)	5.7342(2)	10.249(1)
c (Å)	7.3386(2)	7.2673(8)
α (°)	89.986(1)	90
β (°)	101.040(1)	109.343(4)
γ (°)	100.485(1)	90
V (Å^3)	390.41(2)	761.9(2)
Crystal size (mm^3)	0.055 x 0.152 x 0.204	0.059 x 0.080 x 0.090
Data collection and refinement		
Temperature (K)	298	298
No. of measured reflections	6275	26263
No. of unique reflections	2094	4643
No. Fo > 4σ (Fo)	5348	4634
Range of h, k, l	$-13 \le h \le 13$, $-7 \le k \le 7$, $-10 \le l \le 10$	$-15 \le h \le 15$, $-14 \le k \le 14$, $-10 \le l \le 10$
2θ-max (°)	58.41	61.03
No. parameters	150	280
No. constraints	0	1
$R_{int}/R\sigma$[b]	–/0.022	0.020/0.018
$R1$>4σ (Fo)/$R1$[b]	0.030/0.038	0.013/0.013
w$R2$[b]	0.085	0.035
GoF[b]	1.029	0.936
Min Δ (e/Å^3)	−0.73, 0.73 Å from A^P	−0.39, 0.43 Å from Si4
Max Δ (e/Å^3)	0.81, 0.67 Å from A^P	0.54, 0.65 Å from Ti1

[a] Chemical composition derived from the occupancy factors in the crystal structure refinement and chemical composition used in the discussion after applying site occupancy and charge balance constraints.

[b] $R_{int} = \frac{\sum\left|F_o^2 - F_o^2(\text{mean})\right|}{\sum F_o^2}$, $R_\sigma = \frac{\sum\sigma\left(F_o^2\right)}{\sum F_o^2}$, $R1 = \frac{\sum||Fo|-|Fc||}{\sum|Fo|}$, $wR2 = \left(\frac{\sum w\left(F_o^2 - F_c^2\right)^2}{\sum w\left(F_o^2\right)^2}\right)$, $w = \frac{1}{\left(\sigma\left(F_o^2\right)\right)^2 + (0.0278\cdot P)^2 + 1.35\cdot P}$,

$P = \frac{\max\left(F_o^2, 0\right) + 2\cdot F_c^2}{3}$, $\text{GoF} = \sqrt{\frac{\sum w\left(F_o^2 - F_c^2\right)^2}{n-p}}$, n denotes number of reflections, and p denotes total number of parameters refined.

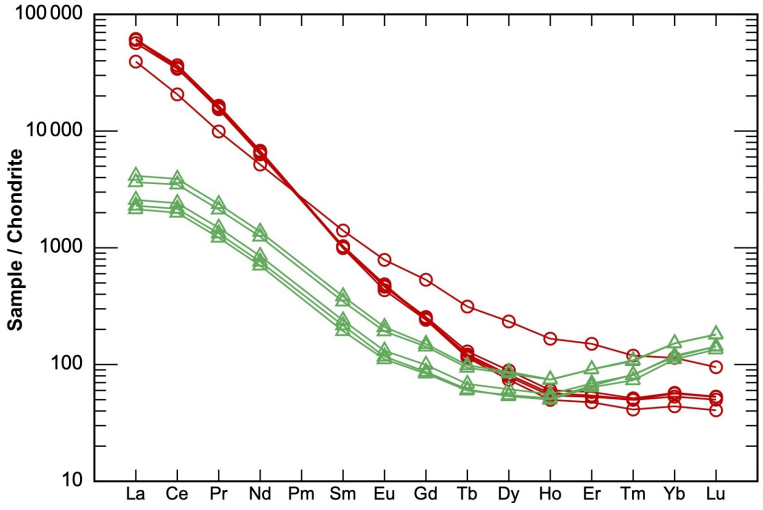

Figure 3. Rare earth element spectra normalized to chondrite (Sun and McDonough, 1989), showing characteristic s shapes for götzenite (red circles) and wöhlerite (green triangles).

Table 5. Bond valence parameters used in Eq. (1) for the calculation of bond valences in Sect. 4.

Bond	R_o	B	Ref	Bond	R_o	B	Ref	Bond	R_o	B	Ref
Na–O	1.695	0.420	(1)	Na–F	1.677	0.37	(2)	Si–O	1.624	0.389	(1)
Ca–O	1.907	0.409	(1)	Ca–F	1.842	0.37	(2)	Ti–O	1.819	0.342	(1)
Ti–F	1.76	0.37	(3)	Mn–O	1.740	0.417	(1)	Mn–F	1.698	0.37	(2)
Fe–O	1.658	0.447	(1)	Fe–F	1.65	0.37	(3)	Sr–O	1.958	0.479	(1)
Sr–F	2.019	0.37	(3)	Zr–O	1.913	0.406	(1)	Zr–F	1.846	0.37	(2)
Nb–O	1.909	0.369	(1)	Nb–F	1.87	0.37	(3)	La–O	2.179	0.359	(1)
La–F	2.024	0.40	(4)	Ce–O	2.114	0.389	(1)	Ce–F	2.036	0.37	(3)
Nd–O	2.103	0.371	(1)	Nd–F	2.008	0.37	(3)				

Ref.: (1) Gagné and Hawthorne (2015), (2) Brown and Altermatt (1985), (3) Brese and O'Keeffe (1991), (4) Zachariasen (1978).

ware Geminography (Nespolo and Ferraris, 2006), confirming the result with some additional information: searching in the lambda region (20, 0, 6), the almost vertical plane was found to be $(\bar{1}04)$, and the twin obliquity was 0.06°, suggesting twinning by reticular pseudo-merohedry with twin index 2, referring to a pseudo-monoclinic I-centered twin lattice with parameters $a = 5.734$ Å, $b = 7.339$ Å, $c = 37.131$ Å, $\alpha = 90.04°$, $\beta = 91.95°$, and $\gamma = 89.99°$. After transformation to the equivalent monoclinic C setting (matrix $-1\ 0\ 1,\ 0\ 1\ 0,\ -1\ 0\ 0$, as given in the International Tables for Crystallography, vol. A; Hahn, 2002), the lattice parameters are $a = 37.37778$ Å, $b = 7.339$ Å, $c = 5.734$ Å, $\alpha = 89.99°$, $\beta = 96.869°$, and $\gamma = 89.962°$, which are very close to those of the above reported C-centered cell that was initially found from the experimental data. Similar calculations with Geminography for a potential reflection twinning on (100) show an obliquity of 1.95° and a twin index 2 (for definitions of twin obliquity and twin index, see Grimmer and Nespolo, 2006). Using initial atomic parameters from Cannillo et al. (1972), the refinement converged with a residual $R1 = 8.2$ %, and all anisotropic displacement parameters were positive within their standard deviations. Rotation twinning on [001] was already observed by Sahama and Hytönen (1957) (after transformation of lattice parameters according to $\boldsymbol{a}+\boldsymbol{b}, \boldsymbol{c}, -\boldsymbol{b}$). Figure 4 shows the resulting arrangement of lattice points for rotation twinning with the observed reciprocal lattice points in Fig. 4a and the lattice points simulated for rotation twinning in Fig. 4b using the software Blender, ver. 4.3.2 (Blender Foundation, 2025). The simulations were limited to ±3 for h, k, and l. In the $l = 2n$ layers in Fig. 4b, the lattice points of the blue domain cover the exactly overlapping lattice points of the red domain, except at the positions where no blue lattice points were generated.

Figure 4a demonstrates nicely that the observed lattice points of the two unit cells related by rotation twinning are almost perfectly aligned in an orientation parallel to b^*, assuming a larger unit cell with monoclinic symmetry. The layers in the 3D reciprocal space patterns, shown to be nearly horizontal, have variable h and k indices and constant l indices. Accordingly, in Fig. 4a and b, with rotation twinning about [001] being assumed for both, in the comparatively sparsely populated layers with $l = 2n$, the spots of both twin compo-

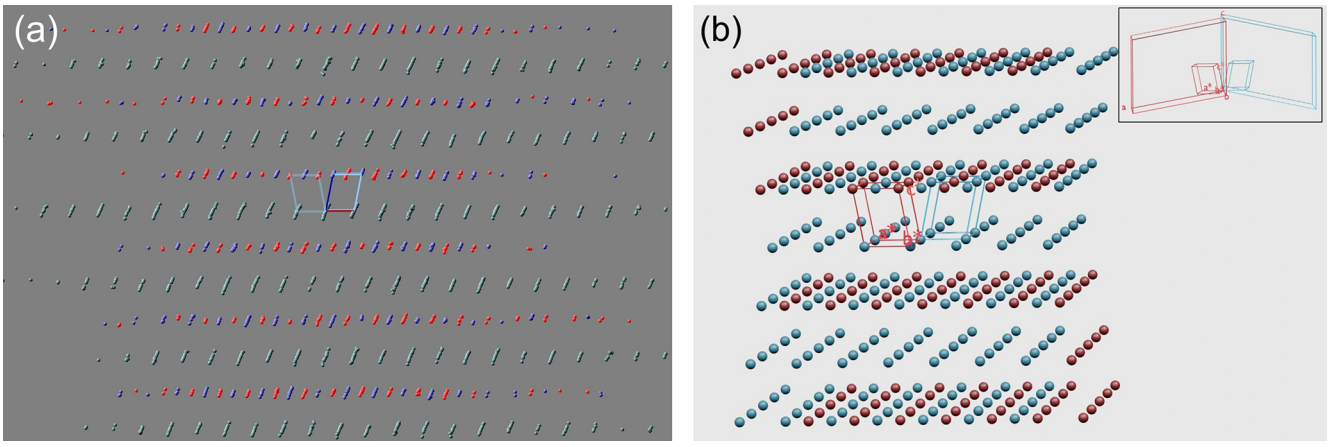

Figure 4. Reciprocal lattice points of götzenite. **(a)** Section of the measured reciprocal space pattern in parallel projection, as viewed almost parallel to b^*. **(b)** Lattice points simulating rotation twinning on [001].

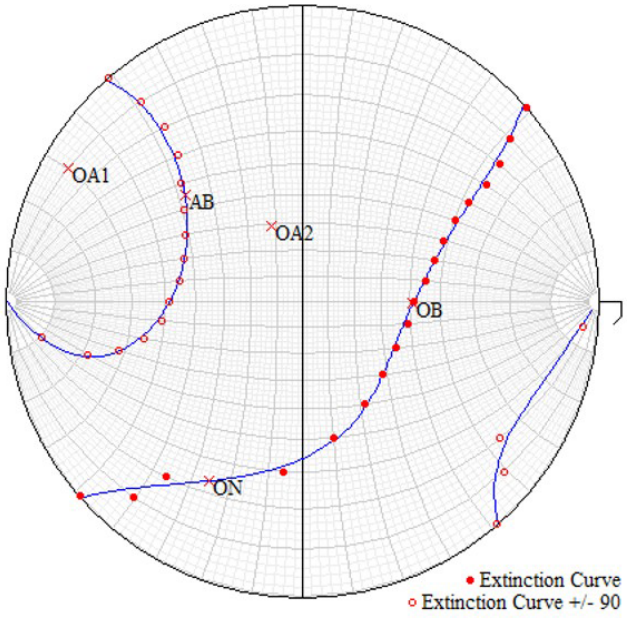

Figure 5. Extinction curves for götzenite. AB denotes acute bisectrix, OB denotes obtuse bisectrix, ON denotes optical normal, and OA1 and OA2 are the optical axes. Filled circles represent the measuring points on the equatorial curve, and open circles are calculated by adding or subtracting 90° from the microscope-stage angle. The blue curves are fitted by least-squares methods.

nents coincide exactly and therefore cannot be distinguished; in the twice as densely populated layers with $l = 2n + 1$, the spots form well-separated alternating rows (red versus blue in 4b), extending along their b^* directions. Overall, the pattern in Fig. 4b perfectly matches the pattern in Fig. 4a, both representing rotation twinning. Consequently, all refinements were done assuming rotation twinning on [001].

Wöhlerite

Another crystal was prepared from the same piece from which the götzenite crystal was obtained (see Fig. 1). SXRD immediately showed that it is not identical to götzenite, revealing reflection twinning on (100) according to $-\boldsymbol{a} - \boldsymbol{c}$, $\boldsymbol{b}$, $\boldsymbol{c}$, with contributions of 31 % and 69 % from the two twin domains, respectively, and with the lattice parameters $a = 10.842(1)$ Å, $b = 10.249(1)$ Å, $c = 7.2673(8)$ Å, and $\beta = 109.343(4)°$ in the monoclinic space group $P2_1$. This corresponds to the symmetry and unit cell parameters of wöhlerite. Assuming and testing rotation twinning on [001] according to $-\boldsymbol{a} - \boldsymbol{c}$, $-\boldsymbol{b}$, $\boldsymbol{c}$ yielded a plausible model as well but resulted in slightly higher residuals. Analyzing the two potential twinning laws for wöhlerite with Geminography, we found pseudo-merohedry for reflection twinning on (100)

with the normal direction [201], obliquity of 0.24°, and twin index 1. Similarly, for rotation twinning on [001], pseudomerohedry was found as well, with $(\bar{1}02)$ for the normal plane, obliquity of 0.24°, and a twin index 1. From these results, [001] and (100) twinning were equivalent. Therefore, due to the slightly better residuals in the crystal structure refinement, reflection twinning is assumed here for the twin model of wöhlerite. Using initial parameters from Biagioni et al. (2012) (ICSD entry no. 187604), the crystal structure could be refined to $R1 = 1.3\,\%$.

2.3 Optical investigations

The optical properties of götzenite were investigated using a microrefractometer spindle stage, as described by Medenbach (1985). It is equipped with a second spindle where a smithsonite crystal ($n_e = 1.8489$, $n_o = 1.6213$) was mounted as an internal refractometer for the exact determination of refractive indices when the match between object crystal and immersion is reached. Extinction curves were recorded by rotating the object spindle in steps of 10° and by reading the microscope stage angles for extinction under crossed polarizers. The same crystal that was used for the single-crystal investigations was also examined optically. The resulting extinction curves are presented in Fig. 5, plotted on a Wulff net, where the great circles (longitudes) represent the spindle angles and the small circles (latitudes) represent the microscope-stage angles. As an example, the optic axis OA1 corresponds to an angle of 10° on the spindle and 150° on the microscope stage. The program EXCALIBRW (Gunter et al., 2005) was used for plotting the extinction curves to determine the orientation of the principal axes of the indicatrix and to determine the optical angle $2V$. Calculation of $2V$ from the refractive indices was done according to $\cos V = \frac{n_x}{n_y}\sqrt{\frac{(n_z+n_y)(n_z-n_y)}{(n_z+n_x)(n_z-n_x)}}$ (Bloss, 1961). Wöhlerite could not be examined optically because of its complex twinning.

In order to measure the refractive indices in the three directions of the main axes (AB, OB, and ON) of the optical indicatrix, the corresponding angles from Fig. 5 were set on the spindle and the microscope stage, pointing north–south parallel to the vibration direction of the polarizer. Then, the refractive index in the respective direction was determined by an iterative process of changing immersion liquids until the crystal became invisible and the Becke line did not move upon moving the microscope stage up and down (changing the focus). In each direction, the resulting refractive index was redetermined using the smithsonite crystal as an internal refractometer directly in the immersion oil.

The total electronic polarizability of minerals and inorganic compounds can be derived from the mean refractive index using the Anderson–Eggleton relationship (Anderson, 1975; Eggleton, 1991):

$$\alpha_{AE} = \frac{\left(n^2-1\right)V_m}{4\pi + \left(\frac{4\pi}{3} - 2.26\right)\left(n^2-1\right)}, \tag{2}$$

with the total electronic polarizability α_{AE} (Å^3); the molar volume V_m (Å^3) of the formula unit; and the mean refractive index n at 589.3 nm, with 2.26 representing the electronic overlap factor (Shannon and Fischer, 2006, 2016). Alternatively, the total electronic polarizability can be calculated from the sum of the individual contributions of cations (α_{cat}) and of anions (α_{an}) in the respective compounds according to

$$\alpha_{tot} = \sum_{i=1}^{Ncat} m_i \cdot \alpha(\text{cat})_{ei} + \sum_{i=1}^{Nan} n_i \cdot \alpha(\text{an})_{ei}, \tag{3}$$

with m cations and n anions of a certain type i. Whereas the cation polarizabilities are strictly additive, the anion polarizabilities α(an) including H_2O molecules are correlated with the volume occupied by the anion expressed by the volume of the formula unit divided by the number of anions according to

$$\alpha_{an} = \alpha^{o}_{-} \cdot 10^{-N_o/V_{an}^{1.2}}, \tag{4}$$

with V_{an} denoting anion molar volume. The individual polarizabilities of cations and the values α^{o}_{-} (free-ion polarizability) and N_o for anions are taken from Tables 4 and 5 in Shannon and Fischer (2016). The mean refractive index n_D at $\lambda = 589.3$ nm is then calculated from the total polarizability using the Anderson–Eggleton relationship solved for n according to

$$n_{AE} = \sqrt{\frac{4\pi\alpha_{AE}}{\left(2.26 - \frac{4\pi}{3}\right)\alpha_{AE} + V_m} + 1}. \tag{5}$$

Alternatively, the mean refractive indices can be calculated following the approach of Gladstone and Dale (1863), adapted to minerals by Mandarino (1976). Using a set of parameters k_i (Gladstone–Dale constants) from Mandarino (1981), a specific chemical refractivity (cm^3 g^{-1}),

$$K_c = \sum_i \frac{k_i p_i}{100}, \tag{6}$$

can be calculated, where p_i denotes the weight percentages of the oxide contents in the respective compounds. This quantity, K_c, is then compared to an experimental physically derived value defined as $K_p = (<n> - 1)/D$, with density denoted by D (Mandarino, 1979, 1981). The "compatibility" measures the agreement between the two sides of the equation $(n-1)/D = \Sigma k_i p_i/100$, where superior is $<2\,\%$, excellent is 2 %–4 %, good is 4 %–6 %, fair is 6 %–8 %, and poor is $>8\,\%$. Replacing K_c in Eq. (6) with K_p allows for the calculation of the mean refractive index according to

$$<n_{GD}> = \sum_i \frac{k_i p_i}{100} \cdot D + 1. \tag{7}$$

Refractive indices derived from electronic polarizabilities and from Gladstone–Dale constants were calculated using the program POLARIO (Fischer et al., 2018).

3 Results

3.1 Götzenite

3.1.1 Chemical composition

Based on the results of EPMA and LA-ICP-MS (see Tables 2, 3, and S1), the resulting chemical formula can be written as $Na_{1.50(7)}Ca_{5.18(11)}Sr_{0.13(3)}Fe^{2+}_{0.03(1)}Mn_{0.014(4)}Zr_{0.06(2)}La_{0.08(1)}Ce_{0.11(2)}Nd_{0.017(2)}TE_{0.021(2)}Ti_{0.80(7)}Nb_{0.18(6)}(Si_2O_7)_2O_{0.9(1)}F_{3.5(2)}$, with the trace elements $TE = Y_{0.002(1)}Pr_{0.008(2)}Ta_{0.0020(7)}Th_{0.007(2)}U_{0.0024(2)}$ and minor traces of Rb, Ba, Eu, Gd, Tb, Dy, Ho, Er, Tm, Yb, Lu, Hf, and Pb at <0.001 atoms per formula unit (apfu). Thus, the following chemical composition is used for further discussion: $Na_{1.50}Ca_{5.18}Sr_{0.13}Fe^{2+}_{0.03}Mn_{0.01}Zr_{0.06}La_{0.08}Ce_{0.11}Nd_{0.02}Ti_{0.81}Nb_{0.19}(Si_2O_7)_2O_{1.2}F_{2.8}$ omitting elements <0.01 apfu. Considering the fact that the sum of O (outside of Si_2O_7) and F, distributed over two sites in the crystal structure, should be limited to 4 apfu and that the chemical composition should be charge balanced, the number of F and O atoms was adjusted within a few standard deviations to meet these criteria. Similarly, the Ti and Nb content was adjusted to 0.81 Ti and 0.19 Nb, respectively, yielding 1 apfu in total. The chemical composition can be compared with the crystal chemical assignments derived from the site occupancies listed in Sect. 4.1.

3.1.2 Crystal structure

After recognizing the twinning and applying the twin law to the dataset, the crystal structure was successfully refined, yielding a residual of $R1 < 3\,\%$, which confirms the basic structural features of götzenite. The atom parameters from the final refinement are listed in Table 6, and interatomic distances are listed in Table 7. The labeling of the sites follows the convention of Sokolova (2006), as described in Sect. 1.2.1. The distribution of cations over the first five sites in Table 6 was based on crystal chemical considerations and a systematic combination of different arrangements to achieve the lowest possible residual. It was assumed that all positions are fully occupied. Occupancies of cations with lower proportions on the M^H and A^P sites were fixed at values close to the corresponding values from EPMA and LA-ICP-MS results, and the occupancy factor of Ca was determined by the difference compared to the full occupancy. Occupancies at the M^o sites were refined. The comparison between the chemical composition from the chemical analysis and the structure refinement shows very good agreement (see Table 4). This agreement and the low residual indicate that the distribution of elements over the cation sites is essentially correct. All displacement parameters could be refined anisotropically, yielding positive and meaningful eigenvalues (mean-square atomic displacements). Anisotropic displacement parameters are listed in Table S3. Whereas the M^H and M^o1 sites are clearly 6-coordinated and the M^o2 site is clearly 8-coordinated, there are some additional distances for A^P and M^o3, extending the coordination by two and one ligand, respectively. A^P has six distances to O and F between 2.35 and 2.54 Å (see Table 7) and two additional bonds to O1 at 2.991(2) and 3.205(2) Å. Since there is a clear gap between the 6-coordinated atoms and the additional ligands, it is still considered to be an octahedral coordination for the crystal–chemical interpretation. For optical studies (see Sect. 2.3 and 4.1), the additional atoms are considered to contribute to the polarizabilities of the A^P cations. The M^o3 site has six distances to F and O between 2.34 and 2.40 Å and one additional bond to O5 with 3.06 Å. This site is considered to be octahedrally coordinated for both crystal–chemical and optical characterization.

3.1.3 Optical properties

Following the procedure described in Sect. 2.3, the refractive indices were determined to be $n_x = 1.662(2)$ (OB), $n_y = 1.663(2)$ (ON), and $n_z = 1.670(2)$ (AB) using a smithsonite crystal as the internal refractometer. The optic axial angle $2V = 61(2)°$ was determined from the extinction curves in Fig. 5, represented by the angle between OA1 and OA2 at the acute bisectrix AB. The corresponding angle calculated from the refractive indices is 42°. Just a slight adjustment of n_x and n_y within half an error yields values exactly corresponding to the measured $2V$, resulting in $n_x = 1.6614$ (OB), $n_y = 1.6636$ (AB), and $n_z = 1.670$ (AB) with an optic angle of $2V = 61°$. The results are discussed and compared with the optical properties of other rinkite-group minerals in Sect. 4.1.

3.2 Wöhlerite

3.2.1 Chemical composition

The chemical formula of wöhlerite is derived from the mean composition of the two EPMA analyses conducted at the University of Freiburg and the University of Bremen for the major elements and from the LA-ICP-MS analyses for the trace elements. The resulting formula can be written as $Na_{1.63(7)}Ca_{4.37(13)}Sr_{0.04(1)}Zr_{0.63(4)}Fe^{2+}_{0.23(2)}Mn_{0.09(1)}Ce_{0.010(3)}Ta_{0.012(1)}TE_{0.01}Nb_{0.79(4)}Ti_{0.20(4)}(Si_2O_7)_2O_{2.54(2)}F_{1.37(9)}$, with the trace elements (TEs) of $Y_{0.0016(3)}La_{0.004(1)}Nd_{0.003(1)}Hf_{0.00218(2)}U_{0.0015(1)}$ and minor traces of Rb, Ba, Pr, Sm, Eu, Gd, Tb, Dy, Ho, Er, Tm, Yb, Lu, Pb, and Th < 0.001 apfu. For discussion, the following chemical composition is used: $Na_{1.63}Ca_{4.37}Sr_{0.04}Zr_{0.63}Fe^{2+}_{0.23}Mn_{0.09}Ce_{0.01}Ta_{0.01}Nb_{0.79}Ti_{0.20}(Si_2O_7)_2O_{2.6}F_{1.4}$, omitting elements < 0.01 apfu and scaling the sum of Nb + Ti to yield 1 apfu and O + F = 4 apfu. The chemical composition can be compared

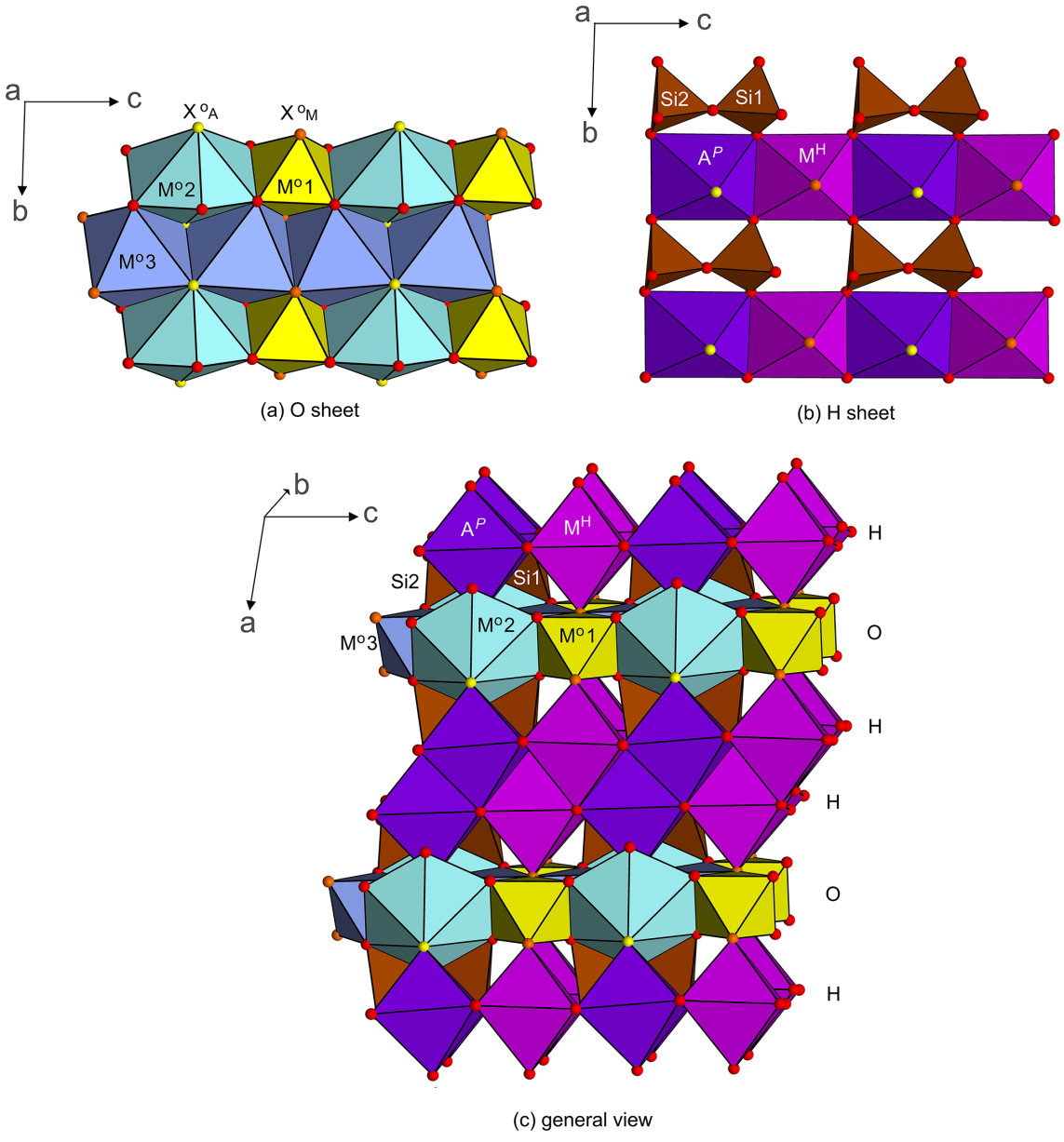

Figure 6. Crystal structure projections of götzenite. **(a)** O sheet with M°1 (Ti, Nb), M°2 (Na, Ca), and M°3 (Ca, Na) polyhedra; **(b)** H sheet with Si_2O_7 groups, A^P (Ca, Sr, Fe, La), and M^H (Ca, Mn, Ce, Nd, Zr) polyhedra; and **(c)** linkage of H and O sheets.

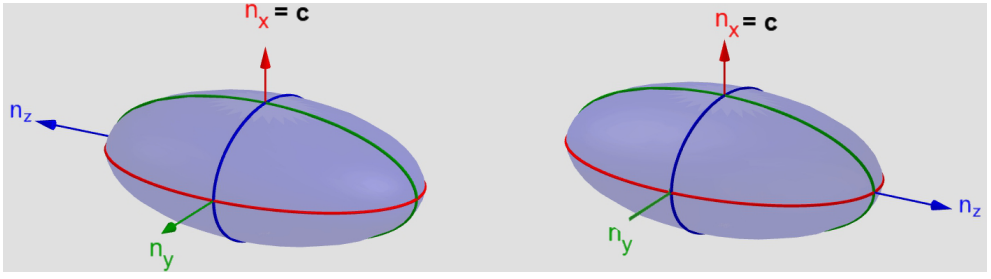

Figure 7. Optical indicatrix of the two twin individuals related to each other by rotation about n_x corresponding to the crystallographic c axis [001]. Drawn with GeoGebra® (2025).

Table 6. Atom parameters of götzenite listing site names after Sokolova (2006), elements for site population, occupancy factors, Wyckoff positions (International Tables for Crystallography (Hahn, 2002)), atomic coordinates, and the equivalent displacement parameters U_{eq}.

Site	Site population	Site occupancies	Wy. pos.	x	y	z	U_{eq} (Å^2)
M^H	Ca,Mn,Ce,Nd,Zr	0.900, 0.005, 0.055, 0.010,0.030	2i	0.63090(4)	0.22767(7)	0.90948(12)	0.0100(1)
A^P	Ca,Sr,Fe,La	0.885, 0.065, 0.015, 0.035	2i	0.63252(5)	0.22794(8)	0.40746(14)	0.0158(1)
M^o1	Ti,Nb	0.468(2), 0.032(2)	2i	−0.0131(3)	0.0240(5)	−0.0041(6)	0.0041(4)
M^o2	Na,Ca	0.742(10), 0.258(10)	1b	0	0	1/2	0.0180(5)
M^o3	Ca,Na	0.660(8), 0.340(8)	2i	0.99338(7)	0.49638(10)	0.24195(8)	0.0171(3)
Si1	Si	1	2i	0.71722(7)	0.75153(12)	0.65187(11)	0.0076(2)
Si2	Si	1	2i	0.72454(8)	0.75572(13)	0.21531(9)	0.0075(2)
O1	O	1	2i	0.7590(2)	0.7867(4)	0.4441(3)	0.0230(4)
O2	O	1	2i	0.6160(2)	0.9413(3)	0.6684(6)	0.0142(5)
O3	O	1	2i	0.6189(2)	0.9360(3)	0.1423(6)	0.0157(5)
O4	O	1	2i	0.6450(3)	0.4796(4)	0.6657(7)	0.0237(5)
O5	O	1	2i	0.6674(3)	0.4807(4)	0.1612(7)	0.0271(5)
O6	O	1	2i	0.8760(2)	0.8134(4)	0.7858(3)	0.0175(4)
O7	O	1	2i	0.8861(2)	0.8361(3)	0.1719(3)	0.0163(4)
X^o_M	F,O	0.55(3), 0.45(3)	2i	0.8856(2)	0.2602(3)	0.9677(5)	0.0143(5)
X^o_A	F	1	2i	0.8869(2)	0.3062(3)	0.4761(5)	0.0189(4)

The isotropic displacement parameter U_{eq} is defined as one-third of the trace of the orthogonalized U_{ij} tensor. The coefficients U_{ij} of the anisotropic displacement factor tensor of the atoms are defined as follows: $-2\pi^2\left[(ha^*)^2U_{11}+\ldots+2hka^*b^*U_{12}+\ldots\right]$.

Table 7. Selected distances (Å) and angles (°) for götzenite.

M^H	– O5	2.282(4)	A^P	– O5	2.352(4)	M^o1	– X^o_M	1.797(3)	M^o2	– X^o_A	2.218(1) 2×
	– O4	2.308(4)		– O4	2.354(4)		– O7	1.967(4)		– O1	2.375(2) 2×
	– O3	2.372(2)		– X^o_A	2.360(2)		– O7	1.968(4)		– O7	2.549(2) 2×
	– X^o_M	2.378(2)		– O2	2.369(2)		– O6	1.969(4)		– O6	2.731(2) 2×
	– O2	2.380(3)		– O2	2.533(3)		– O6	1.980(4)		mean	2.468(2)
	– O3	2.395(3)		– O3	2.536(3)		– X^o_M	2.198(3)			
	mean	2.353(3)		mean	2.417(3)		mean	1.980(4)			
M^o3	– X^o_A	2.336(3)	Si1	– O4	1.599(2)	Si2	– O5	1.596(2)	Si1–O1–Si2		153.8(1)
	– X^o_A	2.346(3)		– O2	1.606(2)		– O3	1.601(2)			
	– X^o_M	2.377(3)		– O6	1.629(2)		– O7	1.630(2)			
	– O7	2.377(2)		– O1	1.653(2)		– O1	1.651(2)			
	– O6	2.385(2)		mean	1.622(2)		mean	1.620(2)			
	– X^o_M	2.401(3)									
	mean	2.370(3)									

with the crystal chemical assignments derived from the site occupancies listed in Sect. 4.2.

3.2.2 Crystal structure

The crystal structure of wöhlerite could be refined to $R1 = 1.3\,\%$ with anisotropic displacement parameters and with all eigenvalues being positive. The atom parameters from the final refinement are listed in Table 8, and interatomic distances are listed in Table 9, with site designations following the designations introduced by Dal Bo et al. (2022) for wöhlerite-group minerals.

4 Discussion

4.1 Götzenite

The chemical composition of götzenite is very complex and resembles the composition of late-stage götzenite from the matrix of the Fohberg phonolite (Spürgin et al., 2024). It is very close to other members in the rinkite group, as shown in Table 10, listing the chemical compositions of götzenites compared with those of fogoite-(Y), batievaite-(Y), hainite-(Y), and bortolanite, all having similar lattice parameters (see Table 11) and being easily confused with götzenite. The close relationship is also reflected by the small distances separating corresponding atoms from each other in the different crys-

Table 8. Atom parameters of wöhlerite, elements for site population, occupancy factors, atomic coordinates, and the equivalent displacement parameters U_{eq}. All atoms are in Wyckoff position 2a (International Tables for Crystallography (Hahn, 2002)).

Site	Site population	Site occupancies	x	y	z	U_{eq} (Å^2)
X1	Zr, Fe, Mn	0.588(8), 0.322(8), 0.090	0.34094(3)	0.24269(3)	0.05379(5)	0.0071(1)
X2	Ca	1	0.34498(6)	0.25512(8)	0.55269(11)	0.0129(2)
X3	Na, Ca	0.743(10), 0.257(10)	0.63036(10)	0.36900(13)	0.44481(20)	0.0151(5)
X4	Ca, Na	0.927(9), 0.073(9)	0.36944(6)	0.86545(8)	0.05333(11)	0.0116(2)
X5	Na, Ca	0.905(9), 0.095(9)	0.87654(14)	0.52373(15)	0.30968(24)	0.0187(5)
X6	Nb, Ti	0.778(4), 0.222(4)	0.13331(3)	0.00691(3)	0.19442(5)	0.00791(8)
X7	Ca	1	0.84623(6)	0.13562(6)	0.30041(10)	0.0104(1)
X8	Ca	1	0.14704(6)	0.63424(6)	0.19874(10)	0.0090(1)
Si1	Si	1	0.08090(8)	0.32657(9)	0.19685(12)	0.0075(2)
Si2	Si	1	0.07360(8)	0.31850(9)	0.63767(14)	0.0078(2)
Si3	Si	1	0.55874(9)	0.06903(9)	0.43635(12)	0.0080(2)
Si4	Si	1	0.43497(8)	0.56557(9)	0.12171(13)	0.0079(2)
O1	O	1	0.0086(2)	0.1891(2)	0.1215(4)	0.0116(4)
O2	O	1	−0.0191(2)	0.1941(2)	0.6163(4)	0.0113(4)
O3	O	1	0.0049(2)	0.4538(2)	0.0855(4)	0.0140(5)
O4	O	1	0.0180(2)	0.4526(2)	0.6968(4)	0.0155(5)
O5	O	1	0.2320(2)	0.3284(2)	0.2038(4)	0.0146(5)
O6	O	1	0.2223(2)	0.2900(3)	0.7786(4)	0.0152(5)
O7	O	1	0.5097(2)	−0.0737(2)	0.3511(4)	0.0143(5)
O8	O	1	0.4599(2)	0.4152(2)	0.0763(4)	0.0150(5)
O9	O	1	0.4717(2)	0.1920(2)	0.3189(4)	0.0133(5)
O10	O	1	0.5392(2)	0.6679(3)	0.0851(4)	0.0174(5)
O11	O	1	0.7105(2)	0.0968(3)	0.4817(4)	0.0184(5)
O12	O	1	0.2912(2)	0.6230(2)	0.0205(4)	0.0135(4)
W1,O13	O	1	0.2445(2)	0.0729(3)	0.0438(4)	0.0152(5)
W2,O14	O, F	0.93(5), 0.07(5)	0.2253(2)	0.0704(2)	0.4405(4)	0.0158(7)
W4,O15	O, F	0.84(5), 0.16(5)	0.2164(2)	0.8459(2)	0.2267(4)	0.0142(6)
O16	O	1	0.0913(3)	0.3489(2)	0.4251(4)	0.0213(5)
O17	O	1	0.5229(2)	0.0798(2)	0.6407(4)	0.0157(4)
W3,F	F	1	0.7617(2)	0.3434(2)	0.2579(3)	0.0131(4)

The isotropic displacement parameter U_{eq} is defined as one-third of the trace of the orthogonalized U_{ij} tensor. The coefficients U_{ij} of the anisotropic displacement factor tensor of the atoms are defined as follows: $-2\pi^2\left[(ha^*)^2U_{11}+\ldots+2hka^*b^*U_{12}+\ldots\right]$.

Table 9. Selected distances (Å) and angles (°) for wöhlerite.

X1	– O13	2.019(3)	X2	– O14	2.287(2)	X3	– F	2.285(2)	X4	– F	2.249(2)
(Zr,	– O10	2.041(2)	(Ca)	– O7	2.306(2)	(Na,	– O15,F	2.427(2)	(Ca,	– O7	2.281(2)
Fe,	– O9	2.045(2)		– O6	2.457(2)	Ca)	– O9	2.459(2)	Na)	– O8	2.393(2)
Mn)	– O6	2.046(2)		– O5	2.537(2)		– O7	2.519(2)		– O15,F	2.401(2)
	– O5	2.051(2)		– O17	2.558(2)		– O14,F	2.557(2)		– O13	2.510(3)
	– O8	2.163(2)		– O9	2.596(2)		– O17	2.670(2)		– O12	2.611(2)
				– O10	2.667(2)		– O8	2.745(2)		– O10	2.694(3)
				– O16	2.767(3)		– O11	2.908(3)			
	mean	2.061(2)		mean	2.522(2)		mean	2.571(2)		mean	2.448(2)
X5	– F	2.190(2)	X6	– O14	1.853(2)	X7	– F	2.298(2)	X8	– O15,F	2.283(2)
(Na,	– O2	2.275(3)	(Nb,	– O15,F	1.857(2)	(Ca)	– O11	2.312(2)	(Ca)	– O2	2.311(2)
Ca)	– O14,F	2.464(2)	Ti)	– O13	1.996(2)		– O12	2.318(2)		– O12	2.340(2)
	– O13	2.518(2)		– O4	2.118(2)		– O2	2.354(2)		– O11	2.356(2)
	– O3	2.570(2)		– O3	2.159(2)		– O4	2.380(2)		– O3	2.373(2)
	– O4	2.818(2)		– O1	2.263(2)		– O1	2.570(2)		– O1	2.445(2)
	– O16	2.836(3)									
	– O6	2.924(3)									
	mean	2.574(2)		mean	2.041(2)		mean	2.372(2)		mean	2.351(2)
Si1	– O3	1.610(2)	Si2	– O2	1.599(2)	Si3	– O11	1.593(2)	Si4	– O12	1.599(2)
	– O1	1.617(2)		– O4	1.615(2)		– O7	1.609(2)		– O8	1.617(2)
	– O5	1.622(2)		– O6	1.625(2)		– O9	1.635(2)		– O10	1.627(3)
	– O16	1.641(2)		– O16	1.648(2)		– O17	1.659(2)		– O17	1.640(2)
	mean	1.623(2)		mean	1.622(2)		mean	1.624(2)		mean	1.621(2)
Si1–O16–Si2		158.5(1)	Si3–O17–Si4		150.5(1)						

Table 10. Comparison of chemical compositions of götzenites and related minerals.

No.	Mineral	Chemical composition[i]	ref[j]
1	götzenite ideal	$NaCa_6Ti(Si_2O_7)_2OF_3$	(1)
2	götzenite Fohberg	$Na_{1.50}Ca_{5.18}Sr_{0.13}Fe_{0.03}Mn_{0.01}Zr_{0.06}La_{0.08}Ce_{0.11}Nd_{0.02}Ti_{0.81}Nb_{0.19}(Si_2O_7)_2O_{1.2}F_{2.8}$	this work
3	götzenite Fohberg	$Na_{1.40}Li_{0.01}K_{0.02}Mg_{0.01}Ca_{4.94}Sr_{0.16}Mn_{0.02}Al_{0.11}Fe^{3+}_{0.05}Zr_{0.02}Ti_{0.83}Nb_{0.13}(Si_2O_7)_2O_{0.47}F_{2.63}(OH)_{0.66}$	(2)
4	götzenite Fohberg[a]	$Na_{1.55(5)}K_{0.01(1)}Ca_{5.01(9)}Sr_{0.18(2)}Fe^{2+}_{0.02(1)}Mn_{0.02(1)}Zr_{0.07(2)}Ti_{0.74(5)}Nb_{0.20(2)}Ce_{0.11(4)}La_{0.07(2)}(Si_2O_7)_2O_{1.03}F_{2.75(7)}$	(3)
5	götzenite Mt. Shaheru	$Na_{1.16}K_{0.02}Ca_{5.52}Mg_{0.05}Mn_{0.01}Fe^{2+}_{0.05}Fe^{3+}_{0.03}Al_{0.62}Ti_{0.90}(Si_2O_7)_2O_{1.12}F_{3.25}Cl_{0.03}(SO_4)_{0.02}(OH)_{0.21}$	(4)
6	götzenite Kola[b]	$Na_{1.67}K_{0.04}Ca_{4.06}Sr_{0.13}Mn_{0.08}Zr_{0.03}Fe^{3+}_{0.04}Al_{0.45}Ti_{1.19}Nb_{0.16}(Si_2O_7)_2O_{1.17}F_{2.86}(OH)_{0.56}$	(5)
7	götzenite Kola[b]	$Na_{1.68}K_{0.08}Ca_{5.51}Sr_{0.10}Mn_{0.24}Zr_{0.02}Fe^{3+}_{0.04}Al_{0.34}Ti_{0.94}Nb_{0.23}(Si_2O_7)_2O_{1.81}F_{3.07}(OH)_{0.91}$	(6)
8	götzenite Kola[b]	$Na_{1.52}K_{0.01}Ca_{5.16}Sr_{0.06}Mg_{0.01}Mn_{0.07}Zr_{0.01}Fe^{2+}_{0.01}Al_{0.07}Ti_{0.81}Nb_{0.19}REE_{0.08}(Si_2O_7)_2O_{0.27}F_{3.58}$	(7)
9	götzenite[b,c] Ukraine	$Na_{1.54}K_{0.06}Ca_{3.78}Sr_{0.08}Mn_{0.06}Zr_{0.06}Fe^{3+}_{0.08}Al_{0.62}TR_{0.05}Ti_{1.02}Nb_{0.04}(Si_2O_7)_2O_{1.06}F_{2.56}(OH)_{0.38}$	(8)
10	götzenite[d,e] Ukraine (malignite)	$Na_{1.65}Ca_{4.41}Sr_{0.17}Mn_{0.07}Zr_{0.27}Fe^{2+}_{0.05}REE_{0.10}Ti_{0.92}Nb_{0.06}(Si_2O_7)_2O_{0.58}F_{3.25}$	(9)
11	götzenite[d,f] Ukraine (juvite)	$Na_{1.56}Ca_{4.73}Sr_{0.17}Mn_{0.08}Zr_{0.19}Fe^{2+}_{0.06}REE_{0.03}Ti_{0.92}Nb_{0.05}(Si_2O_7)_2O_{0.65}F_{3.13}$	(9)
12	götzenite Cupaello (Umbria)	$Na_{1.70}K_{0.12}Ca_{5.20}Sr_{0.14}Mg_{0.15}Mn_{0.02}Fe^{2+}_{0.14}Al_{0.08}Ti_{0.85}(Si_2O_7)_2O_{0.94}F_{2.63}(OH)_{0.23}$	(10)
13	götzenite S. Venanzo (Umbria)	$Na_{1.25}K_{0.04}Ca_{5.23}Sr_{0.02}Mg_{0.14}Mn_{0.01}Zr_{0.36}Fe^{2+}_{0.08}Al_{0.01}Ti_{0.78}Nb_{0.01}REE_{0.02}(Si_2O_7)_2O_{1.58}F_{3.16}$	(10)
14	götzenite Pian di Celle (Umbria)[g]	$Na_{1.21(11)}K_{0.008(5)}Ca_{5.52(20)}Sr_{0.06(1)}Mg_{0.05(2)}Mn_{0.006(2)}Zr_{0.11(7)}Fe^{2+}_{0.05(1)}Ti_{0.88(5)}Nb_{0.011(5)}REE_{0.11(5)}(Si_2O_7)_2O_{0.87}F_{3.19(5)}$	(11)
15	götzenite East Greenland	$Na_{1.59}Ca_{5.10}Sr_{0.02}Mn_{0.12}Zr_{0.09}Fe^{2+}_{0.05}Al_{0.01}Ti_{0.90}Nb_{0.06}Ce_{0.13}Nd_{0.02}Y_{0.06}La_{0.08}Gd_{0.01}(Si_2O_7)_2O_{0.83}F_{3.53}$	(12)
16	götzenite Pian di Celle (Umbria)	$Na_{1.04}Ca_{5.74}Sr_{0.04}Mg_{0.04}Fe^{2+}_{0.04}Zr_{0.10}Ti_{0.78}Ce_{0.04}La_{0.02}(Si_2O_7)_2O_{0.44}F_{3.58}$	(13)
17	zirconian götzenite Pian di Celle (Umbria)	$Na_{1.12}Ca_{5.56}Sr_{0.06}Mg_{0.04}Fe^{2+}_{0.02}Zr_{0.26}Ti_{0.68}Ce_{0.04}La_{0.02}(Si_2O_7)_2O_{0.56}F_{3.30}$	(13)
18	götzenite Nyiragongo[h]	$Na_{1.23(8)}K_{0.008(4)}Ca_{5.54(20)}Mg_{0.028(4)}Fe^{2+}_{0.046(5)}Mn_{0.008(4)}Zr_{0.15(7)}Ti_{0.94(2)}Nb_{0.01(1)}(Si_2O_7)_2O_{0.67}F_{3.56(18)}$	(14)
19	götzenite (Minas Gerais, Brazil)	$Na_{2.05}Ca_{4.23}Sr_{0.06}Zr_{0.44}Fe_{0.02}Mn_{0.12}La_{0.03}Ce_{0.04}Y_{0.02}Dy_{0.01}(Ti_{0.90}Nd^{5+}_{0.10})(Si_2O_7)_2O_{1.05}F_{2.98}$	(15)
20	götzenite (Minas Gerais, Brazil)	$Na_{1.61}Ca_{4.75}Sr_{0.10}Zr_{0.07}Fe_{0.07}Mn_{0.12}La_{0.06}Ce_{0.12}Nd_{0.04}Y_{0.03}Dy_{0.02}(Ti_{0.90}Zr_{0.06}Nb_{0.04})(Si_2O_7)_2O_{0.89}F_{3.04}$	(15)
21	götzenite (Latium, Italy)	$Na_{1.35}Ca_{4.95}Sr_{0.09}Fe_{0.03}Mn_{0.04}La_{0.12}Ce_{0.19}Nd^{3+}_{0.02}Pr_{0.01}Dy_{0.01}(Ti_{0.85}Nd^{5+}_{0.09}Zr_{0.06}Th_{0.02})(Si_2O_7)_2O_{0.91}F_{2.95}$	(15)
22	fogoite-(Y) ideal	$Ca_2Y_2Na_3Ti(Si_2O_7)_2(OF)F_2$	(1)
23	fogoite-(Y)	$Na_{2.81}Ca_{2.00}Mn_{0.31}Zr_{0.11}Fe^{2+}_{0.07}Ti_{0.75}Nb_{0.23}Ta_{0.01}La_{0.01}Ce_{0.03}Nd_{0.03}Sm_{0.02}Gd_{0.08}Dy_{0.08}Er_{0.05}Yb_{0.04}Lu_{0.01}Y_{1.20}(Si_2O_7)_2O_{0.93}F_{2.86}$	(16)
24	batievaite-(Y) ideal	$Ca_2Y_2(H_2O)_2\square Ti(Si_2O_7)_2(OH)_2(H_2O)_2$	(1)
25	batievaite-(Y)	$Na_{0.25}Ca_{3.35}Mn_{0.15}Fe^{3+}_{0.04}Zr_{0.21}Ti_{0.76}Nb_{0.15}La_{0.01}Ce_{0.02}Tm_{0.01}Dy_{0.02}Er_{0.04}Yb_{0.11}Lu_{0.02}Y_{0.81}(Si_{1.955}Al_{0.045}O_7)_2(OH)_{1.56}F_{1.17}(H_2O)_{2.16}$	(17)
26	hainite-(Y) ideal	$(Ca_3Y)Na(NaCa)Ti(Si_2O_7)_2(OF)F_2$	(1)
27	hainite-(Y)	$Na_{1.56}Ca_{3.89}Mn_{0.02}Fe^{2+}_{0.03}Zr_{0.21}Ti_{0.60}Nb_{0.15}REE_{0.24}Y_{0.63}(Si_{1.99}Al_{0.01}O_7)_2O_{1.38}F_{2.60}$	(18)
28	hainite-(Y)	$Na_{2.00}Ca_{4.05}Fe_{0.07}Mn_{0.08}Zr_{0.27}La_{0.03}Y_{0.24}Ce_{0.06}Nd^{3+}_{0.03}Dy_{0.03}Yb_{0.02}Er_{0.02}Pr_{0.01}Lu_{0.01}Sr_{0.01}(Ti_{0.78}Zr_{0.15}Nd^{5+}_{0.06})(Si_2O_7)_2O_{1.01}F_{2.85}$	(15)
29	bortolanite ideal	$Ca_2(Ca_{1.5}Zr_{0.5})Na(NaCa)Ti(Si_2O_7)_2(OF)F_2$	(19)
30	bortolanite Brazil	$Na_{2.00}Ca_{4.12}Mn_{0.16}Fe^{2+}_{0.06}Zr_{0.40}Ti_{0.92}Nb_{0.06}La_{0.03}Ce_{0.06}Nd_{0.02}Gd_{0.01}Hf_{0.01}Y_{0.02}(Si_2O_7)_2O_{0.98}F_{2.71}$	(19)
31	bortolanite Lovozero	$Na_{2.075}Ca_{4.20}Mg_{0.045}Mn_{0.03}Zn_{0.01}Fe_{0.035}Zr_{0.69}Ti_{0.775}Nb_{0.045}Th_{0.005}REE_{0.02}(Si_2O_7)_2O_{0.87}F_{2.21}(OH)_{0.92}$	(20)

[a] Mean composition of 13 analyses. [b] Originally named Ca rinkite. [c] TR denotes I, La, Ce, Pr, Nd, Sm, Gd, Dy, Er, Yb. [d] REE denotes rare earth elements and Y. [e] Mean composition from 37 analyses of götzenites. [f] Mean composition from 24 analyses of götzenites. [g] Mean composition from 11 analyses of götzenite in groundmass (nos. 3 to 12 in Table 2 of Sharygin et al. (1996)). [h] East African Rift; mean composition from five analyses of götzenites. [i] Entries 3, 6, 7, and 8 are calculated from the published weight fractions, and the other compositions are copied from the published unit formulas scaled to four Si atoms per unit cell. If values are given for H_2O^+ and H_2O^-, we assume that H_2O^+ represents structural OH groups and that H_2O^- refers to surface adsorption, thus being ignored in the chemical formulae. [j] (1) Sokolova and Cámara (2017). (2) Czygan (1973). (3) Weisenberger et al. (2014). (4) Sahama and Hytönen (1957). (5) Slepnev (1957). (6) Starynkevich-Borneman (1935). (7) Sahama (1960). (8) Val'ter et al. (1963). (9) Dubyna and Kryvdik (2024). (10) Cundari and Ferguson (1994). (11) Sharygin et al. (1996). (12) Christiansen et al. (2003a). (13) Bellezza et al. (2004b). (14) Andersen et al. (2012). (15) RRUFF (2025). Lafuente et al. (2015). (16) Cámara et al. (2017). (17) Lyalina et al. (2016). (18) Lyalina et al. (2015). (19) Day et al. (2022). (20) Selivanova et al. (2024).

Table 11. Comparison of lattice parameters of götzenites with other triclinic minerals of the rinkite group with similar lattice parameters, where "no." refers to the entry number in Table 10.

No.	Mineral	a (Å)	b (Å)	c (Å)	α (°)	β (°)	γ (°)	Ref.[e]
2	götzenite Fohberg	9.6191(3)	5.7342(2)	7.3386(2)	89.986(1)	101.040(1)	100.485(1)	this work
5	götzenite Mt. Shaheru[a]	9.65(11)	5.74(3)	7.32(3)	90	101(1)	101(1)	(1)
5	götzenite Mt. Shaheru[b]	9.667	5.731	7.334	90	101.05	101.31	(2)
15	götzenite East Greenland[c]	9.6192(7)	5.7249(4)	7.3307(5)	89.921(2)	101.132(2)	100.639(2)	(3)
17	zirconian götzenite Umbria[d]	9.636(3)	5.737(1)	7.341(2)	89.94(2)	101.06(3)	100.74(2)	(4)
19	götzenite (Minas Gerais, Brazil)	9.625(3)	5.732(2)	7.296(2)	89.87(2)	101.06(1)	101.34(1)	(5)
20	götzenite (Minas Gerais, Brazil)	9.589(3)	5.721(2)	7.300(1)	89.82(2)	101.22(2)	100.89(2)	(5)
21	götzenite (Latium, Italy)	9.593(3)	5.714(2)	7.347(2)	89.89(2)	101.16(2)	100.16(2)	(5)
23	fogoite-(Y)	9.575(6)	5.685(4)	7.279(5)	89.985(6)	100.933(4)	101.300(5)	(6)
25	batievaite-(Y)	9.4024(8)	5.5623(5)	7.3784(6)	89.919(2)	101.408(2)	96.621(2)	(7)
27	hainite-(Y)	9.6054(10)	5.6928(6)	7.3344(7)	89.903(2)	101.082(2)	100.830(2)	(8)
28	hainite-(Y)[d]	9.500(4)	5.642(3)	7.228(3)	89.93(2)	101.08(2)	100.84(2)	(5)
30	bortolanite Brazil	9.615(3)	5.725(2)	7.316(2)	89.91(1)	101.14(1)	100.91(1)	(9)
31	bortolanite Lovozero	9.5807(5)	5.6943(4)	7.2813(4)	89.891(5)	100.959(4)	101.241(5)	(10)

[a] Lattice parameters transformed according to $\boldsymbol{a}+\boldsymbol{b}$, $\boldsymbol{c}$, $-\boldsymbol{b}$. [b] Lattice parameters from ref. (1) redetermined. [c] Lattice parameters from Table 2 in online version of Christiansen et al. (2003a) (Table 2 is missing in the PDF version). [d] Lattice parameters transformed according to left-hand transformation $\boldsymbol{a}$, $\boldsymbol{c}$, $\boldsymbol{b}$. [e] References: (1) Sahama and Hytönen (1957), (2) Sahama et al. (1966), (3) Christiansen et al. (2003a), (4) Bellezza et al. (2004b), (5) RRUFF (2025), Lafuente et al. (2015), (6) Cámara et al. (2017), (7) Lyalina et al. (2016), (8) Lyalina et al. (2015), (9) Day et al. (2022), (10) Selivanova et al. (2024).

Table 12. Comparison of the separation (Å) of atoms in minerals relative to götzenite studied here.

Mineral	M^H	A^P	M^o1	M^o2	M^o3	Si[a]	O, F[a]	Mean[b]	Ref[c]	No.[d]
götzenite Fohberg	0	0	0	0	0	0	0	0	this work	2
götzenite Mt. Shaheru	0.131	0.020	0.201	0.000	0.071	0.061	0.076	0.072	(1)	5
götzenite East Greenland	0.007	0.005	0.201	0.000	0.003	0.006	0.010	0.006	(2)	15
zirconian götzenite Umbria	0.038	0.055	0.201	0.000	0.003	0.028	0.034	0.032	(3)	17
fogoite-(Y)	0.072	0.053	0.240	0.000	0.044	0.061	0.090	0.064	(4)	23
batievaite-(Y)	0.273	0.291	0.201	0.000	0.084	0.154	0.207	0.202	(5)	25
hainite-(Y)	0.053	0.046	0.201	0.000	0.027	0.045	0.058	0.046	(6)	27
bortolanite Brazil	0.028	0.016	0.006	0.000	0.008	0.014	0.030	0.019	(7)	30
bortolanite Lovozero	0.122	0.074	0.201	0.000	0.025	0.082	0.081	0.077	(8)	31

[a] Grand mean values for Si atoms at two sites and for O and F atoms at nine sites. [b] Grand mean values for columns M^H; A^P; M^o3; Si; and O, F. [c] (1) Cannillo et al. (1972). (2) Christiansen et al. (2003a). (3) Bellezza et al. (2004b), transformed according to left-hand transformation $\boldsymbol{a}$, $\boldsymbol{c}$, $\boldsymbol{b}$. (4) Cámara et al. (2017). (5) Lyalina et al. (2016). (6) Lyalina et al. (2015). (7) Day et al. (2022). (8) Selivanova et al. (2024). [d] Entry number in Table 10.

tal structures of these minerals. These distances are listed in detail in Table S2, and their mean values are shown in Table 12 for the respective structures relative to the götzenite investigated here. The grand mean value might be used as an indicator for isostructural similarities. This value is calculated from all columns in Table 12, except for M^o1 and M^o2, where most of the values are from special positions (0, 0, 0 and 0, 0, 1/2 , respectively) without any degree of freedom. The grand mean value shows that the crystal structure of the götzenite studied here is very close to that from East Greenland (Christiansen et al., 2003a), with a mean separation of 0.006 Å. However, the overall mean separation between götzenites from different localities is as high as 0.072 Å, whereas it is as low as 0.019 Å when compared to the bortolanite from Brazil. Accordingly, similarly to the case of lattice parameters (see Table 11) , the average positions of the crystallographic sites are too similar to allow for a clear distinction between the minerals listed in Table 12. From Table 10, it is also clear that there are significant spreads in the chemical compositions of götzenites from different localities, which makes the clear identification of götzenite based solely on the chemical composition difficult, even in combination with lattice parameters and average site positions. The main difference between the götzenite studied here and bortolanite lies in the occupation of sites in the H sheet and the O sheet, as shown in Table 13. Bond valence calculations (Table 14) of the götzenite studied here show that the assignment of atom sites to the cations is essentially correct (see discussion in Sect. 2.2.1). $Ca_{1.80}Zr_{0.06}$ in götzenite at the M^H site is replaced by $Ca_{1.56}Zr_{0.41}$ in bortolanite; i.e., götzenite has a lower Zr content as compared with bortolanite. Furthermore, the Na content with 2.03 Na in the O sheet of bortolanite is

Table 13. Comparison of site distribution of cations in götzenites with the structural formulae of other rinkite-group minerals where "No." refers to the entry number in Table 10.

No.	Mineral	M^H	A^P	M^O1	M^O2	M^O3	$(Si_2O_7)_2$	$(X^O_M)_2$	$(X^O_A)_2$	Ref.[d]
1	götzenite ideal	Ca_2	Ca_2	Ti	Na	Ca_2	$(Si_2O_7)_2$	OF	F_2	(1)
2	götzenite Fohberg[a]	$Ca_{1.80}Mn_{0.01}$ $Ce_{0.11}Zr_{0.06}$ $Nd_{0.02}$	$Ca_{1.77}Sr_{0.13}$ $Fe^{2+}_{0.03}$ $La_{0.07}$	$Ti_{0.94}Nb_{0.06}$	$Na_{0.74}Ca_{0.26}$	$Ca_{1.32}Na_{0.68}$	$(Si_2O_7)_2$	$O_{0.91}F_{1.09}$	F_2	this work
5	götzenite Mt. Shaheru[a]	Ca_2	$Ca_{1.2}Na_{0.8}$	Ti	Na	Ca_2	$(Si_2O_7)_2$	O_2	F_2	(2)
15	götzenite East Greenland[a]	$Ca_{1.62}Ce_{0.13}$ $Mn_{0.11}Zr_{0.09}$ $Y_{0.05}$	$Ca_{1.88}Ce_{0.12}$	$Ti_{0.92}Fe^{2+}_{0.05}$ $Nb_{0.03}$	$Na_{0.81}Ca_{0.19}$	$Ca_{1.22}Na_{0.78}$	$(Si_2O_7)_2$	$O_{0.82}F_{1.18}$	F_2	(3)
16	götzenite Umbria[a]	$Ca_{1.86}Zr_{0.14}$	Ca_2	$Ti_{0.94}$	$Na_{0.60}Ca_{0.40}$	$Ca_{1.46}Na_{0.54}$	$(Si_2O_7)_2$	F_2	F_2	(4)
16	götzenite Umbria[b]	$Ca_{1.80}Zr_{0.20}$	Ca_2	$Ti_{0.80}\square_{0.20}$	$Na_{0.50}Ca_{0.50}$	$Ca_{1.30}Na_{0.70}$	$(Si_2O_7)_2$	$F_{1.40}O_{0.40}$ $(OH)_{0.20}$	F_2	(4)
17	zirconian götzenite Umbria[a]	$Ca_{1.72}Zr_{0.28}$	Ca_2	$Ti_{0.98}$	$Na_{0.42}Ca_{0.58}$	$Ca_{1.36}Na_{0.64}$	$(Si_2O_7)_2$	F_2	F_2	(4)
17	zirconian götzenite Umbria[b]	$Ca_{1.74}Zr_{0.26}$	Ca_2	$Ti_{0.68}REE_{0.06}$ $Mg_{0.04}Fe_{0.02}\square_{0.20}$	$Na_{0.46}Ca_{0.54}$	$Ca_{1.28}Na_{0.66}$ $Sr_{0.06}$	$(Si_{2.01}O_7)_2$	F_2	F_2	(4)
22	fogoite-(Y) ideal	Y_2	Ca_2	Ti	Na	Na_2	$(Si_2O_7)_2$	OF	F_2	(1)
23	fogoite-(Y)[a]	Y_2	Ca_2	Ti[c]	Na	Na_2	$(Si_2O_7)_2$	OF	F_2	(5)
23	fogoite-(Y)[b]	$Y_{1.21}Ca_{0.01}$ $REE_{0.35}$ $Mn_{0.16}Zr_{0.11}$ $Fe^{2+}_{0.07}Na_{0.09}$	Ca_2	$Ti_{0.76}Nb_{0.23}$ $Ta_{0.01}$	$Na_{0.96}\square_{0.04}$	$Na_{1.78}$ $Mn_{0.15}\square_{0.07}$	$(Si_2O_7)_2$	$O_{1.12}F_{0.88}$	F_2	(5)
24	batievaite-(Y) ideal	Y_2	Ca_2	Ti	$\square$	$(H_2O)_2$	$(Si_2O_7)_2$	$(OH)_2$	$(H_2O)_2$	(1)
25	batievaite-(Y)[a]	$Y_{0.80}Ca_{0.64}$ $REE_{0.24}Mn_{0.16}$ $Zr_{0.12}Fe^{3+}_{0.04}$	Ca_2	$Ti_{0.76}Nb_{0.15}$ $Zr_{0.09}$	$\square_{0.61}Na_{0.25}$ $(H_2O)_{0.14}$	$(H_2O)_{0.76}$ $Ca_{0.70}\square_{0.54}$	$(Si_2O_7)_2$	$(OH)_{1.56}$ $F_{0.44}$	$(H_2O)_{1.28}$ $F_{0.72}$	(6)
26	hainite-(Y) ideal	Ca(Y,REE)	Ca_2	Ti	Na	NaCa	$(Si_2O_7)_2$	OF	F_2	(1)
27	hainite-(Y)[a]	$Y_{0.66}Ca_{1.06}$ $REE_{0.26}Mn_{0.02}$	Ca_2	$Ti_{0.60}Zr_{0.23}$ $Nb_{0.14}Fe_{0.03}$	$Na_{0.87}Ca_{0.13}$	$Na_{1.22}Ca_{0.78}$	$(Si_2O_7)_2$	$O_{0.94}F_{1.06}$	F_2	(7)
29	bortolanite ideal	$Ca_{1.5}Zr_{0.5}$	Ca_2	Ti	Na	NaCa	$(Si_2O_7)_2$	OF	F_2	(1)
30	bortolanite Brazil[a]	$Ca_{1.50}Zr_{0.50}$	$Ca_{1.88}$ $REE_{0.12}$	$Ti_{0.94}Nb_{0.06}$	$Na_{0.85}Ca_{0.15}$	$Na_{1.18}Ca_{0.60}$ $Mn_{0.16}Fe^{2+}_{0.06}$	$(Si_2O_7)_2$	$O_{1.24}F_{0.76}$	F_2	(8)
30	bortolanite Brazil[b]	$Ca_{1.56}Zr_{0.41}$ $Hf_{0.01}Y_{0.02}$	$Ca_{1.88}Ln_{0.12}$	$Ti_{0.94}Nb_{0.06}$	$Na_{0.85}Ca_{0.15}$	$Na_{1.18}Ca_{0.60}$ $Mn_{0.16}Fe^{2+}_{0.06}$	$(Si_2O_7)_2$	$O_{1.24}F_{0.76}$	F_2	(8)
31	bortolanite Lovozero[a]	$Ca_{1.306}Zr_{0.694}$	$Ca_{1.966}$ $Ce_{0.034}$	$Ti_{0.852}$ $Nb_{0.148}$	$Na_{0.669}$ $Ca_{0.331}$	$Na_{1.002}$ $Ca_{0.998}$	$(Si_2O_7)_2$	$O_{1.04}F_{0.96}$	F_2	(9)
31	bortolanite Lovozero[b]	$Ca_{1.39}Zr_{0.61}$	$Ca_{1.97}Ce_{0.01}$ $Nd_{0.01}Th_{0.01}$	$Ti_{0.78}Zr_{0.08}$ $Nb_{0.05}Mg_{0.05}$ $Fe_{0.04}$	$Na_{0.72}Ca_{0.28}$	$Na_{1.36}Ca_{0.56}$ $Mn_{0.03}Zn_{0.01}$	$(Si_2O_7)_2$	$O_{0.87}F_{0.21}$ $(OH)_{0.92}$	F_2	(9)

[a] Occupancies from structure refinement according to the corresponding entry in the ICSD. [b] Occupancies redistributed by the authors considering the results of chemical analyses. [c] Corrected from Ti_2 to Ti. [d] (1) Day et al. (2022). (2) Cannillo et al. (1972). (3) Christiansen et al., 2003a. (4) Bellezza et al. (2004b). (5) Cámara et al. (2017). (6) Lyalina et al. (2016). (7) Lyalina et al. (2015). (8) Day et al. (2022). (9) Selivanova et al. (2024).

Table 14. Bond valence values (vu) for götzenite.

		O1		O2		O3		O4	O5	O6		O7		X^{o}_{M} [a]		X^{o}_{A}		Σ	exp[b]
M^{H}	Ca			0.32		0.32	0.30	0.38	0.40					0.27					
	Mn			0.22		0.22	0.21	0.26	0.27					0.19					
	Ce			0.51		0.52	0.49	0.61	0.65					0.45					
	Zr			0.32		0.32	0.31	0.38	0.40					0.35					
	Nd			0.47		0.48	0.46	0.58	0.62					0.42					
	av			0.33		0.33	0.31	0.39	0.42					0.28				2.06	2.13
A^{P}	Ca			0.32	0.22	0.22		0.34	0.34							0.25			
	Sr			0.42	0.30	0.30		0.44	0.44							0.40			
	Fe			0.20	0.14	0.14		0.21	0.21							0.15			
	La			0.59	0.37	0.37		0.61	0.62							0.43			
	av			0.34	0.23	0.22		0.35	0.35							0.26		1.75	2.04
$M^{o}1$	Ti									0.63	0.65	0.65	0.65	0.98	0.32				
	Nb									0.83	0.85	0.86	0.85	1.28	0.43				
	av									0.64	0.66	0.66	0.66	1.00	0.32			3.94	4.06
$M^{o}2$	Na	0.20	0.20							0.09	0.09	0.13	0.13			0.23	0.23		
	Ca	0.32	0.32							0.13	0.13	0.21	0.21			0.36	0.36		
	av	0.23	0.23							0.10	0.10	0.15	0.15			0.27	0.27	1.49	1.26
$M^{o}3$	Ca									0.31		0.32		0.27	0.26	0.26	0.26		
	Na									0.19		0.20		0.22	0.16	0.17	0.16		
	av									0.27		0.28		0.25	0.22	0.23	0.22	1.48	1.66
Si1	Si	0.93		1.05				1.07		0.99								4.03	4.00
Si2	Si	0.93				1.06			1.08			0.99						4.05	4.00

Note that av denotes bond valence value averaged according to the respective occupancies. [a] Averaged according to $0.455 \cdot \mathrm{bv(O8)} + 0.545 \cdot \mathrm{bv(F1)}$. [b] Calculated from the oxidation states averaged for the respective occupancies.

Table 15. Comparison of the refractive indices of götzenite with the corresponding values of other rinkite-group minerals.

No.[a]	Mineral	n_x	n_y	n_z	$<n>$	$2V_{meas}$	$2V_{calc}$	Ref[c]	n_{AE}	n_{GD}
2	götzenite	1.662(2)	1.663(2)	1.670(2)	1.665(2)	61(2)°	42°	this work	1.666	1.667
	adjusted	1.6614	1.6636	1.670	1.665	61(2)°	61°	this work		
3	götzenite	1.661	1.663	1.670	1.665		56°	(1)	1.647[d]	1.651[d]
5	götzenite	1.660	1.662	1.670	1.664	52°	53.5°	(2)	1.664	1.693
8	götzenite	1.651	1.653	1.659	1.654	60°	60°	(3)	1.630	1.632
9	götzenite[b]	1.662(2)	1.665(2)	1.672(2)	1.666(2)	62°	67°	(4)	1.641[d]	1.644[d]
23	fogoite-(Y)	1.686(2)	1.690(2)	1.702(5)	1.693(3)	57(1)°	60°	(5)	1.682	1.694
25	batievaite-(Y)	1.745(5)	1.747(5)	1.752(5)	1.748	60(5)°	65°	(6)	1.728	1.731
30	bortolanite	1.673(2)	1.677(2)	1.690(2)	1.680(2)	56(2)°	58.4°	(7)	1.677	1.679

[a] No. refers to the entry number in Table 10. [b] Listed are rounded mean values of a range of indices given in ref (4). [c] (1) Czygan (1973). (2) Sahama and Hytönen (1957). (3) Sahama (1960). (4) Val'ter et al. (1963). (5) Cámara et al. (2017). (6) Lyalina et al. (2016). (7) Day et al. (2022). [d] Molar volume V_m from entry no. 2.

higher than in the corresponding sheet in götzenite, with 1.42 Na per formula unit. The Ti/Nb ratio with 0.94 Ti and 0.06 Nb in the $M^{o}1$ site of götzenite is exactly identical with the corresponding distribution in bortolanite (see Table 13) and is close to the results of the chemical analyses (0.81 Ti and 0.19 Nb in götzenite, 0.92 Ti and 0.06 Nb in bortolanite). In addition, götzenite has a significant amount of Sr (0.13) at the A^{P} site. Therefore, the fine differentiation between the two minerals only depends on minor differences in the chemical compositions.

Crystal structure projections are shown in Fig. 6 with the linkage of polyhedra within the O sheet and the H sheet and the sequence of the two sheets forming the TS block, with the central octahedral sheet O and two adjacent heteropolyhedral sheets H forming the crystal structure. The figures can be directly compared with Fig. 3 in Day et al. (2022) for bortolanite and with Fig. 4 in Cámara et al. (2017) for fogoite-(Y). For further details, especially on systematics and nomenclature, see Sokolova (2006) and Sokolova and Cámara (2013, 2017).

Table 16. Comparison of chemical compositions of wöhlerites.

No.	Wöhlerite	Chemical composition[a]	Ref[q]
1	ideal	$Na_2Ca_4ZrNb(Si_2O_7)_2O_3F$	(1)
2	Fohberg	$Na_{1.63}Ca_{4.37}Sr_{0.04}Zr_{0.63}Fe^{2+}_{0.23}Mn_{0.09}Ce_{0.01}Ta_{0.01}Nb_{0.79}Ti_{0.20}(Si_2O_7)_2O_{2.6}F_{1.4}$	this work
3	Brevik Norway[b,c]	$Na_{2.05}Ca_{3.65}Zr_{0.97}Nb_{0.85}Fe_{0.23}Mn_{0.17}Mg_{0.08}(Si_2O_7)_2O_{3.22}$	(2,3)
4	Brevik Norway	$Na_{1.93}Ca_{3.83}Mg_{0.02}Zr_{1.04}Fe_{0.19}Mn_{0.11}Ce_{0.03}Nb_{0.77}Ti_{0.04}(Si_2O_7)_2O_{2.62}F_{1.25}$	(4,3)
5	Barkevik Norway[b,d]	$Na_{1.94}Ca_{4.06}Zr_{1.03}Nb_{0.76}(Si_2O_7)_2O_{2.37}F_{1.25}$	(5,4)
6	Langesundsfjord Norway[e]	$Na_2Ca_4ZrNb(Si_2O_7)_2O_3F$	(6)
7	Langesundsfjord Norway	$Na_{2.00}Ca_{3.74}\ Zr_{1.04}Fe^{2+}_{0.16}Mn_{0.10}Hf_{0.02}Nb_{0.82}Ti_{0.12}(Si_2O_7)_2(OH)_{2.30}O_{1.55}F_{1.40}$	(7)
8	Barkevik Norway[f]	$Na_2Ca_4ZrNb(Si_2O_7)_2O_3F$	(8)
9	Guyana	$Na_{2.00}Ca_{3.94}Mg_{0.02}Zr_{0.98}Fe_{0.13}Al_{0.01}Mn_{0.15}Nb_{0.78}Ti_{0.01}(Si_2O_7)_2O_{2.36}F_{1.65}$	(9,3)
10	Brevik Norway	$Na_{2.06}Ca_{3.74}Zr_{1.00}Fe^{2+}_{0.16}Mg_{0.04}Mn_{0.10}Y_{0.02}Nb_{0.78}Ti_{0.14}(Si_2O_7)_2O_{2.72}F_{1.23}$	(10)
11	Brevik Norway	$Na_{1.96}Ca_{3.59}Mg_{0.05}Zr_{0.92}Fe_{0.19}Mn_{0.10}Ce_{0.01}Hf_{0.02}Ta_{0.02}Y_{0.04}Nb_{0.72}Ti_{0.12}(Si_2O_7)_2O_{2.40}F_{1.09}$	(3)
12	Guyana	$Na_{1.94}Ca_{3.78}Sr_{0.02}Mg_{0.03}Zr_{0.92}Fe_{0.07}Al_{0.01}Mn_{0.06}Ce_{0.01}Hf_{0.01}Y_{0.01}Nb_{0.85}Ti_{0.10}(Si_2O_7)_2O_{2.71}F_{0.89}$	(3)
13	Angola	$Na_{1.95}Ca_{3.58}Sr_{0.03}Mg_{0.05}Zr_{0.88}Fe_{0.18}Al_{0.04}Mn_{0.17}La_{0.01}Ce_{0.01}Hf_{0.01}Ta_{0.01}Y_{0.01}Nb_{0.63}Ti_{0.20}(Si_2O_7)_2O_{2.27}F_{1.20}$	(3)
14	Mali	$Na_{2.00}Ca_{3.71}Sr_{0.01}Mg_{0.02}Zr_{0.97}Fe_{0.06}Mn_{0.05}Hf_{0.01}Y_{0.01}Nb_{0.97}Ti_{0.03}(Si_2O_7)_2O_{2.95}F_{0.72}$	(3)
15	Oka Quebec	$Na_{1.82}Ca_{3.86}Sr_{0.01}Mg_{0.07}Zr_{0.96}Fe_{0.02}Mn_{0.05}Ta_{0.01}Y_{0.01}Nb_{0.93}Ti_{0.02}(Si_2O_7)_2O_{2.85}F_{0.80}$	(3)
16	Prairie Lake Ontario	$Na_{1.97}Ca_{3.78}Sr_{0.02}Mg_{0.02}Zr_{0.98}Fe_{0.03}Mn_{0.02}Hf_{0.01}Ta_{0.01}Nb_{0.91}Ti_{0.08}(Si_2O_7)_2O_{2.89}F_{0.81}$	(3)
17	Kaiserstuhl[g]	$Na_{1.81}Ca_{4.42}Mg_{0.07}Zr_{0.81}Fe_{0.05}Mn_{0.05}Ce_{0.01}Ta_{0.01}Nb_{0.97}Ti_{0.03}(Si_2O_7)_2O_{3.30}F_{0.68}$	(11)
18	Prairie Lake Ontario[h]	$Na_{1.95}Ca_{4.03}Mg_{0.03}Zr_{0.91}Fe_{0.08}Mn_{0.04}Hf_{0.01}Nb_{0.98}Ti_{0.09}\ (Si_2O_7)_2O_{3.08}F_{1.08}$	(12)
19	Risøya, Norway[i]	$Na_{1.98}Ca_{3.81}Zr_{0.96}Fe_{0.18}Mn_{0.11}Hf_{0.01}Y_{0.02}Nb_{0.76}Ti_{0.12}(Si_2O_7)_2O_{2.37}F_{1.65}$	(13)
20	Trompetholmen, Norway[j]	$Na_{1.94}Ca_{3.85}Zr_{0.97}Fe_{0.16}Mn_{0.15}Ce_{0.01}Hf_{0.02}Nb_{0.72}Ti_{0.16}(Si_2O_7)_2O_{2.32}F_{1.84}$	(13)
21	Låven, Norway	$Na_{2.19}Ca_{3.45}Zr_{1.01}Fe_{0.12}Mn_{0.33}La_{0.01}Ce_{0.03}Nd_{0.01}Y_{0.03}Hf_{0.02}Nb_{0.72}Ti_{0.17}(Si_2O_7)_2O_{2.38}F_{1.85}$	(13)
22	Los Archipelago[k]	$Na_{1.87}Ca_{4.28}Mg_{0.13}Mn_{0.64}Zr_{0.99}Fe_{0.13}REE_{0.08}Nb_{0.55}Ti_{0.18}(Si_2O_7)_2O_{1.32}F_{3.01}$	(14)
23	Monte Somma, Italy[l]	$Na_{1.57}Ca_{4.17}Mn_{0.28}Zr_{1.09}Fe_{0.15}M_{0.10}Nb_{0.56}Ti_{0.10}(Si_2O_7)_2O_{2.17}F_{1.83}$	(15)
24	Monte de Trigo, Brazil[m]	$Na_{2.16}Ca_{3.82}Mn_{0.19}Zr_{1.03}Fe_{0.05}TE_{0.04}Y_{0.02}Hf_{0.02}Ta_{0.02}Nb_{0.85}Ti_{0.14}(Si_2O_7)_2O_{2.96}F_{1.63}$	(16)
25	Itatiaia, Brazil[o]	$Na_{1.88}Ca_{4.06}Sr_{0.03}Mn_{0.23}Ce_{0.01}Zr_{0.90}Fe_{0.07}Nd_{0.01}Th_{0.01}Sm_{0.01}Nb_{0.65}Ti_{0.13}(Si_{1.98}Al_{0.02}O_7)_2O_{2.28}F_{1.56}$	(17)
26	Itatiaia, Brazil[o]	$Na_{2.03}Ca_{3.67}Mn_{0.27}Ce_{0.03}Zr_{0.94}Fe_{0.06}La_{0.03}Y_{0.01}Nd_{0.02}Th_{0.01}Sm_{0.02}Nb_{0.62}Ti_{0.20}(Si_{1.99}Al_{0.01}O_7)_2O_{2.20}F_{1.64}$	(17)
27	Búzios Island, Brazil[o]	$Na_{1.97}Ca_{3.80}Mg_{0.01}Mn_{0.16}Ce_{0.01}Zr_{0.97}Fe_{0.11}Y_{0.03}Hf_{0.01}Nb_{0.83}Ti_{0.13}(Si_2O_7)_2O_{2.70}F_{1.43}$	(18)
28	Stauper Sandefjord N[n]	$Na_{1.89}Ca_{3.89}Mg_{0.05}Mn_{0.10}Zr_{0.94}Fe_{0.18}REE_{0.02}Y_{0.03}Hf_{0.01}Ta_{0.01}Nb_{0.78}Ti_{0.10}(Si_2O_7)_2O_{2.35}F_{1.92}$	(19)
29	Hafallen Sandefjord N[n]	$Na_{1.85}Ca_{4.02}Mg_{0.05}Mn_{0.11}Zr_{0.93}Fe_{0.16}REE_{0.02}Y_{0.03}Hf_{0.01}Ta_{0.01}Nb_{0.70}Ti_{0.10}(Si_2O_7)_2O_{2.08}F_{2.23}$	(19)
30	Håkestad Larvik N[n]	$Na_{1.83}Ca_{3.96}Mn_{0.24}Zr_{0.92}Fe_{0.09}REE_{0.02}Y_{0.03}Hf_{0.02}Ta_{0.01}Nb_{0.72}Ti_{0.13}\ (Si_2O_7)_2O_{2.26}F_{1.95}$	(19)
31	Stålaker Larvik N[n]	$Na_{1.71}Ca_{4.05}Mg_{0.05}Mn_{0.21}Zr_{0.92}Fe_{0.09}REE_{0.03}Y_{0.04}Hf_{0.02}Ta_{0.01}Nb_{0.82}Ti_{0.09}(Si_2O_7)_2O_{2.63}F_{1.67}$	(19)
32	Hedrum Larvik N[n]	$Na_{1.61}Ca_{4.18}Mg_{0.07}Mn_{0.17}Zr_{0.92}Fe_{0.15}REE_{0.02}Y_{0.03}Hf_{0.01}Ta_{0.01}Nb_{0.65}Ti_{0.11}(Si_2O_7)_2O_{2.14}F_{2.08}$	(19)
33	Trompetholmen N[n]	$Na_{1.95}Ca_{3.87}Mg_{0.04}Mn_{0.12}Zr_{0.97}Fe_{0.19}REE_{0.03}Y_{0.03}Hf_{0.01}Ta_{0.01}Nb_{0.72}Ti_{0.11}(Si_2O_7)_2O_{2.31}F_{1.95}$	(19)
34	Store Arøya N[n]	$Na_{1.99}Ca_{3.94}Mg_{0.02}Mn_{0.14}Zr_{0.97}Fe_{0.04}REE_{0.01}Y_{0.01}Hf_{0.02}Ta_{0.01}Nb_{0.67}Ti_{0.22}(Si_2O_7)_2O_{2.22}F_{2.11}$	(19)
35	Aak, Tvedalen, N[n]	$Na_{2.04}Ca_{3.61}Mg_{0.05}Mn_{0.22}Zr_{0.95}Fe_{0.16}REE_{0.03}Y_{0.04}Hf_{0.01}Ta_{0.01}Nb_{0.79}Ti_{0.07}(Si_2O_7)_2O_{2.19}F_{2.06}$	(19)

Table 16. Continued.

No.	Wöhlerite	Chemical composition[a]	Ref[q]
36	Ønna, Langangen, N[n]	$Na_{1.85}Ca_{3.94}Mg_{0.06}Mn_{0.26}Zr_{0.95}Fe_{0.13}REE_{0.03}Y_{0.04}Hf_{0.01}Ta_{0.01}Nb_{0.76}Ti_{0.05}(Si_2O_7)_2O_{2.10}F_{2.52}$	(19)
37	Pauler, Larvik, N[n]	$Na_{1.72}Ca_{4.05}Mg_{0.05}Mn_{0.18}Zr_{0.92}Fe_{0.13}REE_{0.02}Y_{0.04}Hf_{0.03}Ta_{0.01}Nb_{0.75}Ti_{0.07}(Si_2O_7)_2O_{2.32}F_{1.94}$	(19)
38	Bjønnesvegen, N[n]	$Na_{1.90}Ca_{3.90}Mg_{0.05}Mn_{0.09}Zr_{0.96}Fe_{0.14}REE_{0.03}Y_{0.03}Hf_{0.01}Ta_{0.01}Nb_{0.66}Ti_{0.19}(Si_2O_7)_2O_{2.15}F_{2.13}$	(19)
39	Serra do Mar, Brazil[o]	$Na_{1.99}Ca_{3.87}Sr_{0.08}Mg_{0.13}Mn_{0.52}Zr_{0.94}\ Fe_{0.13}Nd_{0.02}Nb_{0.58}Ti_{0.19}(Si_2O_7)_2O_{2.53}F_{1.88}$	(20)
40	Serra do Mar, Brazil[o]	$Na_{2.01}Ca_{3.62}Sr_{0.06}Mg_{0.03}Mn_{0.54}Zr_{0.91}Fe_{0.06}Sm_{0.01}Nb_{0.76}Ti_{0.08}(Si_{1.96}Al_{0.04}O_7)_2O_{2.30}F_{1.75}$	(20)
41	Monte de Trigo, Brazil[p]	$Na_{2.06}Ca_{3.68}Mn_{0.24}Zr_{1.00}Fe_{0.05}Al_{0.01}Y_{0.03}Hf_{0.01}Ta_{0.01}Nb_{0.56}Ti_{0.17}(Si_2O_7)_2O_{1.91}F_{1.87}$	(21)

[a] Chemical composition scaled to four Si pfu except in entries 24, 25, and 39, where the authors assume that the Si site is shared with Al. O is calculated by charge balance. [b] Irrespective of the authors' choice, Si is considered to reside in Si_2O_7 groups. [c] The Ta content reported by Scheerer (1843) is instead Nb (see Mariano and Roeder (1989) for discussion). [d] According to Goßner and Kraus (1933), the chemical composition is based on the analysis of Brögger and Cleve (1890), ref. (4). [e] Locality after ICSD entry no. 20614 is given as "Langesfjord"; it is changed here to "Langesundsfjord". Chemical composition from crystal structure data. [f] Specimen from mineralogical museum with reference to ref. (5), entry no. 5; chemical composition from crystal structure data. [g] Mean composition from four analyses of wöhlerites (cols. 5 to 8 in Table 1 of ref. (11)). [h] The chemical composition refers to the mineral marianoite, which was described by Dal Bo et al. (2022) to be equivalent to wöhlerite. [i] Mean composition from three analyses of wöhlerites (no. 43 to no. 45 in ref (13)). [j] Mean composition from three analyses of wöhlerites (no. 7, no. 10, no. 11, no. 12, no. 19 in ref (13)). [k] REE equates to $Hf_{0.012}Y_{0.032}La_{0.003}Ce_{0.010}Pr_{0.009}Nd_{0.002}Sm_{0.006}Gd_{0.004}Dy_{0.003}Er_{0.001}Yb_{0.005}$. [l] Domain II in "guarinite". M equates to Al, Mg, Sr, Y. [m] TE equates to $Mg_{0.002}Sc_{0.001}La_{0.006}Ce_{0.014}Pr_{0.002}Nd_{0.006}Sm_{0.002}Gd_{0.001}Dy_{0.002}Er_{0.001}Yb_{0.002}Hf_{0.015}Ta_{0.018}W_{0.001}$; see also entry 39 (ref. 21), which refers to the same species. [n] N denotes Norway. For REEs and the exact amount of Ta, see Table 4 in ref. (19). [o] See also ref. (21), where the compositions of the same species are reported. [p] Data reported to be from ref. (16) (see entry 24) for sample mtr01h, but the weight fractions differ in the two references. [q] (1) Dal Bo et al. (2022). (2) Scheerer (1843). (3) Mariano and Roeder (1989). (4) Brögger and Cleve (1890). (5) Goßner and Kraus (1933). (6) Shibaeva and Belov (1962), ICSD no. 20614. (7) RRUFF (2025). Lafuente et al. (2015). (8) Golyshev et al. (1973). (9) unpublished report by Barron, cited after Mariano and Roeder (1989). (10) Mellini and Merlino (1979). (11) Keller et al. (1995). (12) Chakhmouradian et al. (2008). (13) Andersen et al. (2010). (14) Biagioni et al. (2012). (15) Bellezza et al. (2012). (16) Rojas et al. (2016). (17) Melluso et al. (2017). (18) Gomes et al. (2017). (19) Sunde et al. (2018). (20) Guarino et al. (2019). (21) Gomes et al. (2021).

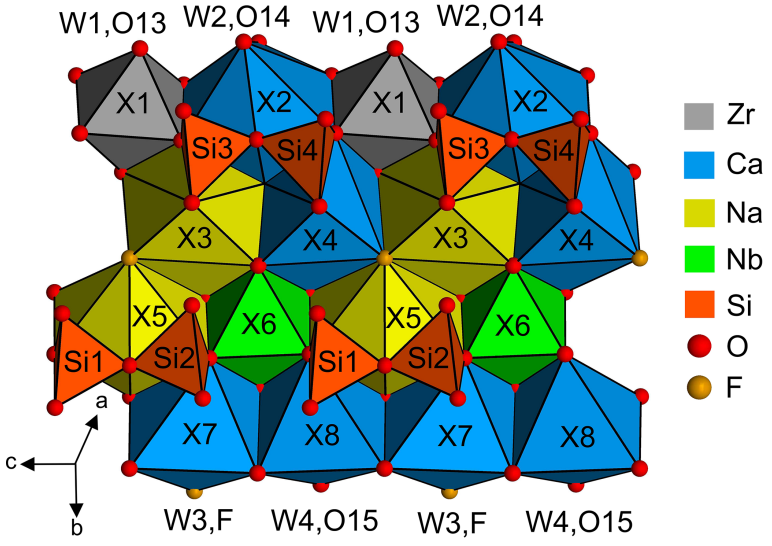

Figure 8. Crystal structure projection of wöhlerite showing the wall of polyhedral linkage and the Si_2O_7 groups.

The refractive indices are compared in Table 15 with the corresponding indices of the other minerals in the rinkite group. In addition, the calculated refractive indices based on the polarizability (n_{AE}) and the Gladstone–Dale approach (n_{GD}) are listed. Deviations between calculated and observed mean refractive indices might indicate problems in the refractive-index measurement or errors in the chemical composition. However, the agreement for the götzenite studied here is excellent, comparing $<n> = 1.665$ with $n_{AE} = 1.666$ and $n_{GD} = 1.667$.

It is remarkable that the crystal could be measured so well at all, given that it is twinned. As shown in Fig. 5, the twinned crystal has proper extinctions in all directions. A second individual cannot be identified under crossed polarizers. The explanation lies in the special position of the n_x axis of the indicatrix being parallel to the crystallographic ***c*** direction. Figure 7 shows the optical indicatrices for the two twin individuals. Since the twin domains are related to each other by rotation about the ***c*** axis, the optical properties are related as well by rotation about n_x. The dimensions of the ellipsoid in Fig. 7 are overemphasized in the main directions to demonstrate that the cross-sections are identical after rotating the indicatrix by 180° about ***c***. Generally, the axes do not have a vector direction. The arrows in Fig. 7 are just drawn

Table 17. Comparison of lattice parameters of wöhlerites, with no. referring to the entry number in Table 16.

No.	Locality	a (Å)	b (Å)	c (Å)	β (°)	Ref.[c]
2	Fohberg	10.8419(12)	10.2489(12)	7.2673(8)	109.343(4)	this work
5	Barkevik Norway	10.80	10.26	7.26	109.05	(1)
6	Langesundsfjord Norway	10.80	10.26	7.26	108.95	(2)
7	Langesundsfjord Norway	10.816(2)	10.239(1)	7.2907(4)	109.04(1)	(3)
8	Barkevik Norway	10.818(3)	10.264(3)	7.282(2)	108.67	(4)
10	Brevik Norway	10.823(3)	10.244(3)	7.290(2)	109.00(4)	(5)
18	Prairie Lake Ontario[a]	10.8459(15)	10.2260(14)	7.2727(10)	109.332(3)	(6)
22	Los Archipelago[b]	10.80498(16)	10.25458(13)	7.28606(10)	109.1168(6)	(7)
23	Monte Somma, Italy	10.836(1)	10.270(1)	7.296(1)	109.13(3)	(8)

[a] The lattice parameters refer to the mineral marianoite, which was described by Dal Bo et al. (2022) to be equivalent with wöhlerite. [b] The authors list $P2_111$ as a space group, but the lattice parameters obviously refer to $P12_11$. [c] References: (1) Goßner and Kraus (1933); (2) Shibaeva and Belov (1962); (3) RRUFF (2025); Lafuente et al. (2015); (4) Golyshev et al. (1973); (5) Mellini and Merlino (1979); (6) Chakhmouradian et al. (2008); (7) Biagioni et al. (2012); (8) Bellezza et al. (2012).

Table 18. Comparison of the separation (Å) of atoms in wöhlerites relative to the wöhlerite studied here, grouped for sites predominantly occupied by certain cations.

Locality	Ca	Nb	Zr	Na	Si	O, F	Grand mean	Ref[a]	No.[b]
Fohberg								this work	2
Langesundsfjord Norway	0.059	0.055	0.193	0.133	0.304	0.368[c]	0.185	(1)	6
Barkevik Norway	0.057	0.041	0.051	0.083	0.032	0.058	0.054	(2)	8
Brevik Norway	0.020	0.027	0.013	0.033	0.023	0.029	0.024	(3)	10
Prairie Lake Ontario	0.014	0.009	0.020	0.013	0.016	0.028	0.017	(4)	18
Los Archipelago	0.029	0.077	0.026	0.037	0.027	0.047	0.040	(5)	22
Monte Somma, Italy	0.027	0.044	0.021	0.027	0.029	0.043	0.032	(6)	23

[a] (1) Shibaeva and Belov (1962). (2) Golyshev et al. (1973). (3) Mellini and Merlino (1979). (4) Chakhmouradian et al. (2008). (5) Biagioni et al. (2012). (6) Bellezza et al. (2012). [b] Entry number in Table 16. [c] Omitting O17, which was misplaced by Shibaeva and Belov (1962).

to indicate the rotation for didactic reasons. This means that the extinction positions determined by the cross-sections are identical in both twin domains. Consequently, the refractive indices are equal in all directions for both twin domains. This distinguishes the crystal examined here from the götzenite studied by Sahama and Hytönen (1957), where n_x is inclined toward the twin axis $\boldsymbol{c}$ ($\boldsymbol{b}$ in the setting of Sahama and Hytönen (1957), thus generating different refractive indices for the same direction in the two twin components. In total, optical data for five götzenites and for fogoite-(Y), batievaite-(Y), and bortolanite are known. The götzenites have mean refractive indices in the range between 1.664 and 1.666, whereas fogoite-(Y) (1.693), batievaite-(Y) (1.748), and bortolanite (1.680) have slightly higher values.

Summarizing, the minerals götzenite, fogoite-(Y), batievaite-(Y), and bortolanite are isostructural and are essentially distinguished by their chemical compositions, which, however, might just be determined by the local availability of elements during growth. In the case of bortolanite and götzenite, the distinction relies on very subtle differences in the composition, and it would not surprise us if a continuous miscibility between these minerals were to exist. Therefore, from a structural point of view, the distinction of the various minerals seems to be somewhat arbitrary.

4.2 Wöhlerite

The identification of wöhlerite based on the chemical composition and the crystal structure is clear, in contrast to that of götzenite, which is isostructural with several other rinkite-group minerals, with differences related to only slight changes in the site occupancies. Wöhlerite has a distinct crystal structure, classified by Merlino and Perchiazzi (1988) as type 8 with unit cell type II, also discussed by Dal Bo et al. (2022). Therefore, the chemical compositions and structural data are listed only for wöhlerites including marianoite (Chakhmouradian et al., 2008), described by Dal Bo et al. (2022) to be equivalent to wöhlerite. The chemical compositions of wöhlerites from various localities are listed in Table 16, scaled to four Si (two Si_2O_7 groups) for direct comparison, except for a few entries where the authors assume Si to be shared with 4-coordinated Al. Accordingly, the chemical composition of wöhlerite can be given in the following range for the major elements: $Na_{1.57–2.19}Ca_{3.45–4.42}Zr_{0.63–1.09}Nb_{0.55–0.98}$

$Ti_{0.01–0.22}(Si_2O_7)_2O_{1.32–3.30}F_{0.68–3.01}$. The wöhlerite from Fohberg studied here is in the low-Na (1.63 Na) and high-Ca (4.37 Ca) region of this range. Variations in the chemical composition do not appear to have a significant influence on the lattice parameters, which are in the range $a =$ 10.80–10.85 Å, $b = 10.23$–10.27 Å, $c = 7.26$–7.29 Å, and $\beta = 108.7$–$109.3°$, as listed in Table 17.

The first crystal structure description of wöhlerite was published by Shibaeva and Belov (1962). They determined the basic principles of the structure, except for one oxygen atom bridging Si3 and Si4. Golyshev et al. (1973) found that just one oxygen atom (O_2, corresponding to the designation by Shibaeva and Belov, 1962) had to be shifted by one-half in the ***c*** direction to be placed correctly together with the reassignment of cation sites. Crystal structure refinements by Mellini and Merlino (1979), Chakhmouradian et al. (2008) (marianoite), and Biagioni et al. (2012) essentially confirmed the structure model. The atom coordinates are listed for comparison in Table S4. Since the origin is not fixed in space group $P12_11$, the average shift in the y coordinates was calculated for every structure to yield the minimum deviation in the ***b*** direction. The corresponding shift vectors are given in the footnote of Table S4. In two cases (no. 7 and no. 17 in Table S4), it was necessary to apply a shift of one-half in the ***c*** and ***a*** directions as well. Finally, the distances to the atom positions for the wöhlerite studied here were calculated and are summarized in Table 18 for atom sites predominantly occupied by certain cations. The grand mean values show that the closest similarity to the wöhlerite studied here is represented by the crystal structure of marianoite described by Chakhmouradian et al. (2008). The site occupancies for all wöhlerite structures are listed in Table 19. Bond valence calculations (see Table 20) show that the assignment of atom sites of the wöhlerite studied here is essentially correct (see discussion in Sect. 2.2.1). A crystal structure projection of wöhlerite is shown in Fig. 8 representing the connection scheme of coordination polyhedra. This can be directly compared with the idealized representation of this wall in Fig. 2 of Dal Bo (2022). There and in other crystal structure descriptions (Shibaeva and Belov, 1962; Golyshev et al., 1973; Chakhmouradian et al., 2008), the polyhedra are represented in an idealized octahedral coordination. In Fig. 8, the polyhedra correspond to the coordination as listed in Table 9; i.e., the coordination numbers are X1 (Zr, Fe, Mn) = 6, X2 (Ca) = 8, X3 (Na, Ca) = 8, X4 (Ca, Na) = 7, X5 (Na, Ca) = 8, X6 (Nb, Ti) = 6, X7 (Ca) = 6, and X8 (Ca) = 6.

Twinning on the orthopinacoid was already mentioned by Brögger and Cleve (1890) to be a common feature in wöhlerite. Mariano and Roeder (1989) mentioned complex lamellar twinning in some of the crystals, and Bellezza et al. (2012) observed twinning on (100), with [001] as the twin axis. As described in Sect. 2.2.2.2, we found reflection twinning on (100) according to $-\boldsymbol{a}-\boldsymbol{c}$, $\boldsymbol{b}$, $\boldsymbol{c}$ and rotation twinning on [001] according to $-\boldsymbol{a}-\boldsymbol{c}$, $-\boldsymbol{b}$, $\boldsymbol{c}$, with a slight preference for reflection twinning yielding a refinement with a final R1

Table 19. Comparison of site distributions[a] of cations in wöhlerites, where no. refers to the entry number in Table 16.

No.	Locality	X1	X2	X3	X4	X5	X6	X7	X8	Ref.[d]
1	ideal	Zr_2	Ca_2	Na_2	Ca_2	Na_2	Nb_2	Ca_2	Ca_2	
2	Fohberg	$Zr_{1.18}Fe_{0.64}Mn_{0.18}$	Ca_2	$Na_{1.49}Ca_{0.51}$	$Ca_{1.85}Na_{0.15}$	$Na_{1.81}Ca_{0.19}$	$Nb_{1.56}Ti_{0.44}$	Ca_2	Ca_2	(1)
6	Langesundsfjord Norway	Ca_2	ZrNb	Ca_2	Na_2	Na_2	ZrNb	Ca_2	Ca_2	this work
8	Barkevik Norway	Zr_2	Ca_2	Na_2	Ca_2	Na_2	Nb_2^b	Ca_2	Ca_2	(2)
10	Brevik Norway	Zr_2	Ca_2	Na_2	Ca_2	Na_2	$Nb_{1.6}Ti_{0.4}$	Ca_2	$Ca_{1.48}Mn_{0.20}Fe_{0.32}$	(3)
18	Prairie Lake Ontario	$Nb_{1.04}Zr_{0.96}$	Ca_2	Na_2	Ca_2	Na_2	$Nb_{1.04}Zr_{0.96}$	Ca_2	Ca_2	(4)
22	Los Archipelago	$Zr_{1.84}Mn_{0.16}$	Ca_2	$Na_{1.80}Ca_{0.20}$	Ca_2	$Na_{1.60}Ca_{0.40}$	$Nb_{1.02}Mn_{0.40}Ti_{0.34}Mg_{0.24}$	Ca_2	$Ca_{1.28}Mn_{0.52}Fe_{0.20}$	(5)
23	Monte Somma, Italy	Zr_2	Ca_2	$Na_{1.60}Ca_{0.40}$	Ca_2	$Na_{1.54}Ca_{0.46}$	$Nb_{1.14}Zr_{0.86}^c$	Ca_2	$Ca_{1.64}Fe_{0.36}$	(6)
		$(Si_2O_7)_4$	W1	W2	W3	W4				(7)
1	ideal	$(Si_2O_7)_4$	O_2	O_2	F_2	O_2				ref.[d]
2	Fohberg	$(Si_2O_7)_4$	O_2	$O_{1.86}F_{0.14}$	F_2	$O_{1.68}F_{0.32}$				(1)
6	Langesundsfjord Norway[a]	$(Si_2O_7)_4$	F_2	O_2	O_2	O_2				this work
8	Barkevik Norway[a]	$(Si_2O_7)_4$	O_2	O_2^b	F_2	O_2				(2)
10	Brevik Norway[a]	$(Si_2O_7)_4$	O_2	$O_{1.6}F_{0.4}$	F_2	O_2				(3)
18	Prairie Lake Ontario[a]	$(Si_2O_7)_4$	O_2	O_2	F_2	O_2				(4)
22	Los Archipelago[c]	$(Si_2O_7)_4$	OF	OF	F_2	OF				(5)
23	Monte Somma, Italy	$(Si_2O_7)_4$	O_2	O_2	F_2	O_2				(6)
										(7)

[a] Site occupancies from corresponding entries in the ICSD. [b] The O : F ratio in the W2 site depends on the Nb : Zr ratio in the X6 site. Here, ideal composition is assumed, yielding full occupancies by Nb and O. [c] Ir is $Nb_{1.14}Mn_{0.86}$ in ref. (7). [d] (1) Dal Bo et al. (2022). (2) Shibaeva and Belov (1962). (3) Golyshev et al. (1973). (4) Mellini and Merlino (1979). (5) Chakhmouradian et al. (2008). (6) Biagioni et al. (2012). (7) Bellezza et al. (2012).

Table 20. Bond valence values (vu) for wöhlerite.

		O1	O2	O3	O4	O5	O6	O7	O8	O9	O10	O11	O12	W1	W2[a]	W3	W4[b]	O16	O17	Σ	Exp[c]
X1	Zr					0.71	0.72		0.54	0.72	0.73			0.77							
	Fe					0.42	0.42		0.32	0.42	0.43			0.45							
	Mn					0.47	0.48		0.36	0.48	0.49			0.51							
	av					0.59	0.60		0.45	0.60	0.61			0.64						3.51	3.18
X2	Ca					0.21	0.26	0.38		0.19	0.16				0.39			0.12	0.20	1.91	2.00
X3	Ca							0.22	0.13	0.26		0.09			0.20	0.30	0.27		0.16		
	Na							0.14	0.08	0.16		0.06			0.13	0.19	0.17		0.10		
	av							0.16	0.09	0.19		0.06			0.14	0.22	0.19		0.11	1.18	1.26
X4	Ca							0.40	0.31		0.15		0.18	0.23		0.33	0.29				
	Na							0.25	0.19		0.09		0.11	0.14		0.21	0.18				
	av							0.39	0.30		0.14		0.17	0.22		0.32	0.28			1.83	1.93
X5	Ca		0.41	0.20	0.11		0.08							0.22	0.25	0.39		0.10			
	Na		0.25	0.13	0.07		0.05							0.14	0.13	0.25		0.07			
	av		0.27	0.13	0.07		0.06							0.15	0.14	0.26		0.07		1.15	1.10
X6	Nb	0.38		0.51	0.57									0.79	1.16		1.13				
	Ti	0.27		0.37	0.42									0.60	0.90		0.87				
	av	0.36		0.48	0.53									0.75	1.10		1.08			4.29	4.78
X7	Ca	0.20	0.34		0.32							0.37	0.37			0.29				1.88	2.00
X8	Ca	0.27	0.37	0.32								0.33	0.35				0.38			2.02	2.00
Si1	Si	1.02		1.04		1.01												0.96		4.02	4.00
Si2	Si		1.07		1.02		1.00											0.94		4.03	4.00
Si3	Si							1.04		0.97		1.08							0.91	4.01	4.00
Si4	Si								1.02		0.99		1.07						0.96	4.04	4.00

Note that av denotes bond valence value averaged according to the respective occupancies. [a] Averaged according to $0.93 \cdot bv(O) + 0.07 \cdot bv(F)$. [b] Averaged according to $0.84 \cdot bv(O) + 0.16 \cdot bv(F)$. [c] Calculated from the oxidation states averaged for the respective occupancies.

value as low as 1.3 %. However, it is entirely possible that both types of twinning might occur.

5 Conclusion

Our studies showed that götzenite and wöhlerite coexist in the Fohberg phonolite (Kaiserstuhl, SW Germany). Both minerals show a complex twinning as revealed by single-crystal X-ray diffraction studies. Götzenite represents a special case of twinning, where the twin domains are arranged in a certain way such that one of the main axes of the optical indicatrix is parallel to the crystallographic ***c*** axis in both domains, thus showing unique extinction under the polarizing microscope. Götzenite is isostructural with several other rinkite-group minerals (see Table 10) with similar lattice parameters (see Table 11) and differences only in terms of slight changes in the site occupancies (see Tables 12 and 13) in contrast to wöhlerite having a distinct crystal structure.

Data availability. CSD contains the supplementary crystallographic data (deposition numbers 2524183 for götzenite and 2524397 for wöhlerite) for this paper. These data can be obtained free of charge from FIZ Karlsruhe via https://www.ccdc.cam.ac.uk/structures (provided in: January 2026).

Supplement. The supplement related to this article is available online at https://doi.org/10.5194/ejm-38-75-2026-supplement.

Author contributions. RXF: organizing the project, crystal-structure refinements, comparative studies, writing (original draft). JB: sample preparation, single-crystal X-ray diffraction, twin models. GB: collecting samples. LAF: electron probe micro-analysis. AK: electron probe micro analysis and laser ablation inductively coupled plasma mass spectrometry. SN: optical measurements. SiS: providing samples, pre-characterization by powder X-ray diffraction, petrological description.

Competing interests. The contact author has declared that none of the authors has any competing interests.

Disclaimer. Publisher's note: Copernicus Publications remains neutral with regard to jurisdictional claims made in the text, published maps, institutional affiliations, or any other geographical representation in this paper. The authors bear the ultimate responsibility for providing appropriate place names. Views expressed in the text are those of the authors and do not necessarily reflect the views of the publisher.

Acknowledgements. We thank Giovanni Ferraris and an anonymous reviewer for their comments on the paper, Michael Fischer (Bremen) for the fruitful discussions, and Olaf Medenbach (Bochum) for providing the equipment for the optical measurements.

Financial support. The article processing charges for this open-access publication were covered by the University of Bremen.

Review statement. This paper was edited by Sergey Krivovichev and reviewed by Giovanni Ferraris and one anonymous referee.

References

Andersen, T., Erambert, M., Larsen, A. O., and Selbekk, R. S.: Petrology of nepheline syenite pegmatites in the Oslo Rift, Norway: Zirconium silicate mineral assemblages as indicators of alkalinity and volatile fugacity in mildly agpaitic magma, J. Petrol., 51, 2303–2325, https://doi.org/10.1093/petrology/egq058, 2010.

Andersen, T., Elburg, M., and Erambert, M.: Petrology of combeite- and götzenite-bearing nephelinite at Nyiragongo, Virunga Volcanic Province in the East African Rift, Lithos, 152, 105–121, https://doi.org/10.1016/j.lithos.2012.04.018, 2012.

Anderson, O. L.: Optical properties of rock-forming minerals derived from atomic properties, Fortschr. Mineral., Special Issue IMA papers, 52, 611–629, 1975.

Bellezza, M., Franzini, M., Larsen, A. O., Merlino, S., and Perchiazzi, N.: Grenmarite, a new member of the götzenite-seidozerite-rosenbuschite group from the Langesundsfjord district, Norway: definition and crystal structure, Eur. J. Mineral., 16, 971–978, https://doi.org/10.1127/0935-1221/2004/0016-0971, 2004a.

Bellezza, M., Merlino, S., and Perchiazzi, N.: Chemical and structural study of the Zr,Ti-disilicates in the venanzite from Pian di Celle, Umbria, Italy, Eur. J. Mineral., 16, 957–969, https://doi.org/10.1127/0935-1221/2004/0016-0957, 2004b.

Bellezza, M., Merlino, S., and Perchiazzi, N.: Distinct domains in "guarinite" from Monte Somma, Italy: Crystal structures and crystal chemistry, Can. Mineral., 50, 531–548, https://doi.org/10.3749/canmin.50.2.531, 2012.

Belsky, A., Hellenbrandt, M., Karen, V. L., and Luksch, P.: New developments in the Inorganic Crystal Structure Database (ICSD): accessibility in support of materials research and design, Acta Crystallogr., B58, 364–369, https://doi.org/10.1107/s0108768102006948, 2002.

Biagioni, C., Merlino, S., Parodi, G. C., and Perchiazzi, N.: Crystal chemistry of minerals of the wöhlerite group from the Los Archipelago, Guinea, Can. Mineral., 50, 593–609, https://doi.org/10.3749/canmin.50.3.593, 2012.

Blender Foundation: Blender 5.0, Amsterdam, http://www.blender.org, last access: March 2025.

Bloss, F. D.: An introduction to the methods of optical crystallography, Holt, Rinehart and Winston, New York, USA, ISBN 0-03-010220-0, 1961.

Bosi, F.: Bond valence at mixed occupancy sites. I. Regular polyhedra, Acta Crystallogr., B70, 864–870, https://doi.org/10.1107/S2052520614017855, 2014.

Brese, N. E. and O'Keeffe, M.: Bond-valence parameters for solids, Acta Crystallogr., B47, 192–197, https://doi.org/10.1107/S0108768190011041, 1991.

Brögger, W. C. and Cleve, P. T.: Die Mineralien der Syenitpegmatitgänge der südnorwegischen Augit- und Nephelinsyenite. II. Metasilicate, Zeitschrift für Krystallographie und Mineralogie, 16, 294–520, 1890.

Brown, I. D. and Altermatt, D.: Bond-valence parameters obtained from a systematic analysis of the Inorganic Crystal Structure Database, Acta Crystallogr., B41, 244–247, https://doi.org/10.1107/S0108768185002063, 1985.

Cámara, F., Sokolova, E., Abdu, Y. A., Hawthorne, F. C., Charrier, T., Dorcet, V., and Carpentier, J. F.: Fogoite-(Y), $Na_3Ca_2Y_2Ti(Si_2O_7)_2OF_3$, a Group I TS-block mineral from the Lagoa do Fogo, the Fogo volcano, São Miguel Island, the Azores: description and crystal structure, Mineral. Mag., 81, 369–381, https://doi.org/10.1180/minmag.2016.080.103, 2017.

Cámara, F., Sokolova, E., and Hawthorne, F. C.: From structure topology to chemical composition. XII. Titanium silicates: the crystal chemistry of rinkite, Na_2Ca_4*REE*$Ti(Si_2O_7)_2OF_3$, Mineral. Mag., 75, 2755–2774, https://doi.org/10.1180/minmag.2011.075.6.2755, 2011.

Cannillo, E., Mazzi, F., and Rossi, G.: Crystal structure of götzenite, Sov. Phys. Crystallogr., 16, 1026–1030, 1972.

Chakhmouradian, A. R. and Mitchell, R. H.: Marianoite, a new member of the cuspidine group from the prairie lake silicocarbonatite, Ontario: reply, Can. Mineral., 47, 1280–1282, https://doi.org/10.3749/canmin.47.5.1280, 2009.

Chakhmouradian, A. R., Mitchell, R. H., Burns, P. C., Mikhailova, Y., and Reguir, E. P.: Marianoite, a new member of the cuspidine group from the prairie lake silicocarbonatite, Ontario, Can. Mineral., 46, 1023–1032, https://doi.org/10.3749/canmin.46.4.1023, 2008.

Chirvinskiy, P. N.: Tr. Kol'sk. bazy Akad. Nauk SSSR, 1, 82, 1935.

Christiansen, C. C., Johnsen, O., and Makovicky, E.: Crystal chemistry of the rosenbuschite group, Can. Mineral., 41, 1203–1224, https://doi.org/10.2113/gscanmin.41.5.1203, 2003a.

Christiansen, C. C., Gault, R. A., Grice, J. D., and Johnsen, O.: Kochite, a new member of the rosenbuschite group from the Werner Bjerge alkaline complex, East Greenland, Eur. J. Mineral., 15, 551–554, https://doi.org/10.1127/0935-1221/2003/0015-0551, 2003b.

Christiansen, C. C. and Rønsbo, J. G.: On the structural relationship between götzenite and rinkite, Neues Jb. Miner. Monat., 2000, 496–506, 2000.

Cundari, A. and Ferguson, A. J.: Appraisal of the new occurrence of $götzenite_{ss}$, khibinskite and apophyllite in kalsilite-bearing lavas from San Venanzo and Cupaello (Umbria), Italy, Lithos, 31, 155–161, https://doi.org/10.1016/0024-4937(94)90006-X, 1994.

Czygan, W.: Götzenit, ein komplexes Ti-Zr-Silikat aus dem Kaiserstuhl, Berichte der Naturforschenden Gesellschaft zu Freiburg im Breisgau, 63, 5–12, 1973.

Dal Bo, F., Friis, H., and Mills, S. J.: Nomenclature of wöhlerite-group minerals, Mineral. Mag., 86, 661–676, https://doi.org/10.1180/mgm.2022.10, 2022.

Dal Bo, F., Friis, H., Elburg, M. A., Hatert, F., and Andersen, T.: Pilanesbergite: a new rock-forming mineral occurring in nepheline syenite from the Pilanesberg Alkaline Complex, South Africa,

Eur. J. Mineral., 36, 73–85, https://doi.org/10.5194/ejm-36-73-2024, 2024.

Day, M. C., Sokolova, E., Hawthorne, F. C., Horváth, L., and Pfenninger-Horvát, E.: Bortolanite, $Ca_2(Ca_{1.5}Zr_{0.5})Na(NaCa)Ti(Si_2O_7)_2(FO)F_2$, a new rinkite-group (seidozerite supergroup) TS-block mineral from the Bortolan Quarry, Poços de Caldas Massif, Minas Gerais, Brazil, Can. Mineral., 60, 699–712, https://doi.org/10.3749/canmin.2200001, 2022.

Dubyna, O. V. and Kryvdik, S. G.: Götzenite in the nepheline syenites of the Pokrovo-Kyriyivo massif (Azov area, Ukraine) (in Ukrainian), Mineralogical Journal (Ukraine), 46, 19–34, https://doi.org/10.15407/mineraljournal.46.02.019, 2024.

Eggleton, R. A.: Gladstone-Dale constants for the major elements in silicates: Coordination number, polarizability, and the Lorentz-Lorentz relation, Can. Mineral., 29, 525–532, 1991.

Farrugia, L. J.: WinGX suite for small-molecule single-crystal crystallography, J. Appl. Crystallogr., 32, 837–838, https://doi.org/10.1107/S0021889899006020, 1999.

Ferraris, G.: Modular structures – the paradigmatic case of the heterophyllosilicates, Z. Kristallogr., 223, 76–84, https://doi.org/10.1524/zkri.2008.0005, 2008.

Fischer, R. X. and Messner, T.: STRUPLO, https://www.brass.uni-bremen.de, last access: March 2025.

Fischer, R. X., Burianek, M., and Shannon, R. D.: POLARIO, a computer program for calculating refractive indices from chemical compositions, Amer. Mineral., 103, 1345–1348, https://doi.org/10.2138/am-2018-6587, 2018.

Fleischer, M.: New mineral names – götzenite, Amer. Mineral., 43, 790–791, 1958a.

Fleischer, M.: New mineral names – rinkite, johnstrupite, rinkolite, lovchorrite, and calcium rinkite (all = mosandrite), Amer. Mineral., 43, 795–796, 1958b.

Gagné, O. C. and Hawthorne, F. C.: Comprehensive derivation of bond-valence parameters for ion pairs involving oxygen. Acta Crystallogr., B71, 562–578, https://doi.org/10.1107/S2052520615016297, 2015

GeoGebra®: Apps und Materialien, http://www.geogebra.org, last access: January 2025.

Gladstone, J. H. and Dale, T. P.: Researches on the refraction, dispersion, and sensitiveness of liquids, Philos. Trans. Roy. Soc. London, 153, 317–343, https://doi.org/10.1098/rstl.1863.0014,1863.

Golyshev, V. M., Otroshchenko, L. P., Simonov, V. I., and Belov, N. V.: Refining the atomic structure of wöhlerite, $NaCa_2(Zr,Nb)[Si_2O_7](F,O)_2$, Soviet Physics Doklady, 18, 287–289, 1973.

Gomes, C. d. B., Alves, F. R., Azzone, R. G., Rojas, G. E. E., and Ruberti, E.: Geochemistry and petrology of the Búzios Island alkaline massif, SE, Brazil, Brazilian Journal of Geology, 47, 127–145, https://doi.org/10.1590/2317-4889201720160121, 2017.

Gomes, C. d. B., Azzone, R. G., Rojas, G. E. E., Guarino, V., and Ruberti, E.: Agpaitic alkaline rocks in Southern Brazilian Platform: A review, Minerals, 11, 1–30, https://doi.org/10.3390/min11090934, 2021.

Goßner, B. and Kraus, O.: Die chemische Zusammensetzung von Wöhlerit, Z. Kristallogr., 86, 308–310, 1933.

Grimmer, H. and Nespolo, M.: Geminography: the crystallography of twins, Z. Kristallogr., 221, 28–50, https://doi.org/10.1524/zkri.2006.221.1.28, 2006.

Guarino, V., Gennaro, R. D., Melluso, L., Ruberti, E., and Azzone, R. G.: The transition from miaskitic to agpaitic rocks, as highlighted by the accessory phase assemblages in the Passa Quatro Alkaline Complex, Can. Mineral., 57, 339–361, https://doi.org/10.3749/canmin.1800073, 2019.

Gunter, M. E., Downs, R. T., Bartelmehs, K. L., Evans, S. H., Pommier, C. J. S., Grow, J. S., Sanchez, M. S., and Bloss, F. D.: Optic properties of centimeter-sized crystals determined in air with the spindle stage using EXCALIBRW, Amer. Mineral., 90, 1648–1654, https://doi.org/10.2138/am.2005.1892, 2005.

Hahn, T.: International Tables for Crystallography, Vol A Space-group Symmetry, Kluwer Academic Publishers, ISBN 0-7923-6590-9, 2002.

Jochum, K. P., Willbold, M., Raczek, I., Stoll, B., and Herwig, K.: Chemical characterisation of the USGS reference glasses GSA-1G, GSC-1G, GSD-1G, GSE-1G, BCR-2G, BHVO-2G and BIR-1G using EPMA, ID-TIMS, ID-ICP-MS and LA-ICP-MS, Geostandards and Geoanalytical Research, 29, 285–302, https://doi.org/10.1111/j.1751-908X.2005.tb00901.x, 2005.

Keller, J., Williams, C. T., and Koberski, U.: Niocalite and wöhlerite from the alkaline and carbonatite rocks at Kaiserstuhl, Germany, Mineral. Mag., 59, 561–566, https://doi.org/10.1180/minmag.1995.059.396.18, 1995.

Lafuente, B., Downs, R. T., Yang, H., and Stone, N.: The power of databases: the RRUFF project. Highlights in Mineralogical Crystallography, edited by: Armbruster, T. and Danisi, R. M., Berlin, Germany, W. De Gruyter, 1–30, https://doi.org/10.1515/9783110417104-003, 2015.

Lyalina, L., Zolotarev Jr., A., Selivanova, E., Savchenko, Y., Zozulya, D., Krivovichev, S., and Mikhailova, Y.: Structural characterization and composition of Y-rich hainite from Sakharjok nepheline syenite pegmatite (Kola Peninsula, Russia), Mineral. Petrol., 109, 443–451, https://doi.org/10.1007/s00710-015-0377-3, 2015.

Lyalina, L. M., Zolotarev Jr., A. A., Selivanova, E. A., Savchenko, Y. E., Krivovichev, S. V., Mikhailova, Y. A., Kadyrova, G. I., and Zozulya, D. R.: Batievaite-(Y), $Y_2Ca_2Ti[Si_2O_7]_2(OH)_2(H_2O)_4$, a new mineral from nepheline syenite pegmatite in the Sakharjok massif, Kola Peninsula, Russia, Mineral. Petrol., 110, 895–904, https://doi.org/10.1007/s00710-016-0444-4, 2016.

Mandarino, J. A.: The Gladstone-Dale relationship – Part I: Derivation of new constants, Can. Mineral., 14, 498–502, 1976.

Mandarino, J. A.: The Gladstone-Dale relationship – Part III: Some general applications, Can. Mineral., 17, 71–76, 1979.

Mandarino, J. A.: The Gladstone-Dale relationship – Part IV. The compatibility concept and its application, Can. Mineral., 19, 441–450, 1981.

Mariano, A. N. and Roeder, P. L.: Wöhlerite: Chemical composition, cathodoluminescence and environment of crystallization, Can. Mineral., 27, 709–720, 1989.

Medenbach, O.: A new microrefractometer spindle-stage and its application, Fortschr. Mineral., 63, 111–133, 1985.

Mellini, M. and Merlino, S.: Refinement of the crystal structure of wöhlerite, Tschermaks Mineral. Petrogr. Mitt., 26, 109–123, https://doi.org/10.1007/BF01081296, 1979.

Melluso, L., Guarino, V., Lustrino, M., Morra, V., and Gennaro, R. D.: The REE- and HFSE-bearing phases in the Itatiaia alkaline complex (Brazil) and geochemical evolution of feldspar-rich felsic melts, Mineral. Mag., 81, 217–250, https://doi.org/10.1180/minmag.2016.080.122, 2017.

Merlino, S. and Mellini, M.: Marianoite, a new member of the cuspidine group from the Prairie Lake silicocarbonatite, Ontario: discussion, Can. Mineral., 47, 1275–1279, https://doi.org/10.3749/canmin.47.5.1275, 2009.

Merlino, S. and Perchiazzi, N.: Modular mineralogy in the cuspidine group of minerals, Can. Mineral., 26, 933–943, 1988.

Mills, S. J., Dal Bo, F., Alves, P., Friis, H., and Missen, O. P., Madeiraite, IMA 2021-077, CNMNC Newsletter 64, Mineral. Mag., 85, 181, https://doi.org/10.1180/mgm.2021.93, 2021.

Miyawaki, R., Hatert, F., Pasero, M., and Mills, S. J.: IMA Commission on New Minerals, Nomenclature and Classification (CNMNC) – Newsletter 57, Eur. J. Mineral., 32, 495–499, https://doi.org/10.5194/ejm-32-495-2020, 2020.

Nespolo, M. and Ferraris, G.: The derivation of twin laws in non-merohedric twins. Application to the analysis of hybrid twins, Acta Crystallogr., A62, 336–349, https://doi.org/10.1107/S0108767306023774, 2006.

Neumann, H.: Contributions to the mineralogy of Norway. No. 13. Rosenbuschite and its relation to götzenite, Norsk Geologisk Tidsskrift, 42, 179–186, 1962.

Pautov, L. A., Agakhanov, A. A., Karpenko, V. Y., Uvarova, Y. A., Sokolova, E., and Hawthorne, F. C.: Rinkite-(Y), $Na_2Ca_4YTi(Si_2O_7)_2OF_3$, a seidozerite-supergroup TS-block mineral from the Darai-Pioz alkaline massif, Tien-Shan mountains, Tajikistan: Description and crystal structure, Mineral. Mag., 83, 373–380, https://doi.org/10.1180/mgm.2018.122, 2019.

Pouchou, J. L. and Pichoir, F.: Quantitative analysis of homogeneous or stratified microvolumes applying the model "PAP", in: Electron Probe Quantitation, edited by: Heinrich, K. F. J. and Newbury, D. E., Springer, Boston, 31–75, https://doi.org/10.1007/978-1-4899-2617-3_4, 1991.

Rojas, G. E. E., Ruberti, E., Azzone, R. G., and Gomes, C. D. B.: Eudialyte-group minerals from the Monte de Trigo alkaline suite, Brazil: composition and petrological implications, Braz. J. Geol., 46, 411–426, https://doi.org/10.1590/2317-4889201620160075, 2016.

RRUFF: Database, https://www.rruff.net/, last access: November 2025.

Sahama, T. G.: Identity of calcium rinkite and götzenite, Amer. Mineral., 45, 221–224, 1960.

Sahama, T. G. and Hytönen, K.: Götzenite and combeite, two new silicates from the Belgian Congo, Mineral. Mag., 31, 503–510, 1957.

Sahama, T. G., Saari, E., and Hytönen, K.: Relationship between götzenite and rosenbuschite, Comptes Rendus de la Société Géologique de Finlande, 38, 135–144, 1966.

Scheerer, T.: Ueber den Wöhlerit, eine neue Mineralspecies, Annalen der Physik und Chemie, 59, 327–336, 1843.

Selivanova, E. A., Pakhomovsky, Y. A., Lyalina, L. M., Kompanchenko, A. A., Mikhailova, J. A., and Zolotarev, A. A.: Hydroxyl-bearing bortolanite from the Lovozero alkaline massif, Kola Peninsula, Russia, Mineral. Mag., 88, 380–391, https://doi.org/10.1180/mgm.2024.36, 2024.

Shannon, R. D. and Fischer, R. X.: Empirical electronic polarizabilities in oxides, hydroxides, oxyfluorides, and oxychlorides, Phys. Rev., B73, 235111, https://doi.org/10.1103/PhysRevB.73.235111, 2006.

Shannon, R. D. and Fischer, R. X.: Empirical electronic polarizabilities of ions for the prediction and interpretation of refractive indices: oxides and oxysalts, Amer. Mineral., 101, 2288–2300, https://doi.org/10.2138/am-2016-5730, 2016.

Sharygin, V. V., Stoppa, F., and Kolesov, B. A.: Zr-Ti disilicates from the Pian di Celle volcano, Umbria, Italy, Eur. J. Mineral., 8, 1199–1212, 1996.

Sheldrick, G. M.: SHELXL-97, a program for crystal structure refinement, University of Goettingen, 1997.

Sheldrick, G. M.: A short history of SHELX, Acta Crystallogr., A64, 112–122, https://doi.org/10.1107/s0108767307043930, 2008.

Shibaeva, R. P. and Belov, N. V.: Crystal structure of wöhlerite, $Ca_2Na(Zr,Nb)[Si_2O_7](O,F))_2$, Dokl. Acad. Nauk SSSR, 146, 897–900, 1962.

Slepnev, Y. S.: The minerals of the rinkite group, Izvestiya Akademii Nauk SSSR, Ser. Geol., 3, 63–75, 1957.

Sokolova, E.: From structure topology to chemical composition. I. Structural hierarchy and stereochemistry in titanium disilicate minerals, Can. Mineral., 44, 1273–1330, https://doi.org/10.2113/gscanmin.44.6.1273, 2006.

Sokolova, E. and Cámara, F.: From structure topology to chemical composition. XVI. New developments in the crystal chemistry and prediction of new structure topologies for titanium disilicate minerals with the TS block, Can. Mineral., 51, 861–891, https://doi.org/10.3749/canmin.51.6.861, 2013.

Sokolova, E. and Cámara, F.: The seidozerite supergroup of TS-block minerals: nomenclature and classification, with change of the following names: rinkite to rinkite-(Ce), mosandrite to mosandrite-(Ce), hainite to hainite-(Y) and innelite-1*T* to innelite-1*A*, Mineral. Mag., 81, 1457–1484, https://doi.org/10.1180/minmag.2017.081.010, 2017.

Sokolova, E. and Hawthorne, F. C.: From structure topology to chemical composition. V. Titanium silicates: crystal chemistry of nacareniobsite-(Ce), Can. Mineral., 46, 1333–1342, https://doi.org/10.3749/canmin.46.5.1333, 2008.

Sokolova, E. and Hawthorne, F. C.: From structure topology to chemical composition. XIV. Titanium silicates: refinement of the crystal structure and revision of the chemical formula of mosandrite, $(Ca_3REE)[(H_2O)_2Ca_{0.5}\square_{0.5}]Ti(Si_2O_7)_2(OH)_2(H_2O)_2$, a Group-I mineral from the Saga mine, Morje, Porsgrunn, Norway. Mineral. Mag., 77, 2753–2771, https://doi.org/10.1180/minmag.2013.077.6.05, 2013.

Spürgin, S., Weisenberger, T. B., and Marković, M.: Zeolite-group minerals in phonolite-hosted deposits of the Kaiserstuhl Volcanic Complex, Germany, Amer. Mineral., 104, 659–670, https://doi.org/10.2138/am-2019-6831, 2019.

Spürgin, S., Wilke, F. D. H., Weisenberger, T. B., Hauri, J., Scheu, B., and Kaliwoda, M.: Niobium-rich götzenite as indicator for the evolution of a phonolitic melt, Fohberg, Kaiserstuhl, Germany. Abstract volume, 22nd Swiss Geoscience Meeting, Basel, https://geoscience-meeting.ch/sgm2024/wp-content/uploads/abstract_books/SGM_2024_Symposium_02.pdf (last access: July 2025), 2024.

Starynkevich-Borneman, I. D.: Data on the Geochemistry of the Khibiny Tundra, Mater. k geokhimii Khibinskikh tundr, 1935, 44, 1935.

Sun, S. S. and McDonough, W. F.: Chemical and isotopic systematics of oceanic basalts: implications for mantle composition and processes. Geological Society, London, Special Publications, 42, 313–345, 1989.

Sunde, Ø., Friis, H., and Andersen, T.: Variation in major and trace elements of primary wöhlerite as an indicator of the origin of pegmatites in the Larvik Plutonic Complex, Norway, Can. Mineral., 56, 529–542, https://doi.org/10.3749/canmin.1700050, 2018.

Val'ter, A. A., Yeremenko, G. K., and Stremovskiy, A. M.: Calcium rinkite from alkalic rocks of the Ukraine, Dokl. Acad. Nauk SSSR, 150, 112–115, 1963.

Weisenberger, T. B., Spürgin, S., and Lahaye, Y.: Hydrothermal alteration and zeolitization of the Fohberg phonolite, Kaiserstuhl Volcanic Complex, Germany, Int. J. Earth Sci., 103, 2273–2300, https://doi.org/10.1007/s00531-014-1046-1, 2014.

Wills, A. S.: VaList – Bond valence calculation and listing, Version 4.0.7, available from http://fermat.chem.ucl.ac.uk/spaces/willsgroup/software/valist-bond-valence-calculations-listing/, last access: 2018.

Zachariasen, W. H.: Bond lengths in oxygen and halogen compounds of d and f elements, Journal of the Less-Common Metals, 62, 1–7, https://doi.org/10.1016/0022-5088(78)90010-3, 1978.